

I

A  $\Lambda^0$ -FRAGMENT DECAY IN A CLOUD CHAMBER

II

EXAMPLE OF THE ASSOCIATED PRODUCTION  
OF A  $E^-$  AND TWO  $\theta^0$  PARTICLES

III

A STUDY OF MULTIPLE V-EVENTS

Thesis by

John David Sorrels

In Partial Fulfillment of the Requirements

for the Degree of

Doctor of Philosophy

California Institute of Technology

Pasadena, California

1956

## ACKNOWLEDGEMENTS

The data on which this thesis is based was obtained from the California Institute of Technology 48-inch magnet cloud chambers. These chambers are part of an extensive experimental apparatus designed and built under the direction of Professor C. D. Anderson, Dr. R. B. Leighton, and Dr. E. W. Cowan. Active in the entire construction program were Victor Van Lint, Carl Rouse, Arnold Strassenburg, and George Trilling.

Dr. R. B. Leighton has supervised most of the author's research work relating to this thesis. Dr. C. D. Anderson, who directs the entire CalTech cosmic ray research program, has been stimulating with his advice and discussions.

To all members of the cosmic ray group during the years 1951 to 1955 who contributed to the research described in this paper, the author wishes to express his sincere gratitude.

## ABSTRACT

A cloud chamber photograph of the decay in flight of a heavy nuclear fragment is described. The event is most reasonably interpreted as the decay of a  $\Lambda^0$  particle bound to a  $\text{He}^3$  nucleus, and is similar to examples previously observed in nuclear emulsions. Under this interpretation, the lifetime of the excited fragment in this single example is  $5.4 \pm .6 \times 10^{-10}$  sec and the binding energy of the  $\Lambda^0$  to  $\text{He}^3$  is probably less than 2 Mev.

In another cloud chamber event, a negative cascade particle and two neutral heavy mesons appear to be produced in a single nuclear interaction above a cloud chamber. It is suggested that this event may be an example of the associated production of a  $\Xi^-$  particle with two  $\theta^0$  particles according to the scheme of Gell-Mann.

All of the 48-inch magnet cloud chamber events where two or more V-particles appear to come from a single origin and decay in a single chamber are described. These V-events are analyzed for origin coplanarity and associated production. In the case of  $V^0$ - $V^0$  production, a search for angular relationships between decay planes and the plane containing the lines of flight of the two  $V^0$  detects no strong correlations. Origin coplanarity tests do not indicate three body decay except in two cases of anomalous  $\theta^0$ . The data is consistent with the assumption of associated production of  $\Lambda^0$  with  $\theta^0$ ,  $V^-$  with  $\theta^0$ , and  $V^+$  with  $\Lambda^0$ . The role of the anomalous  $\theta^0$  in multiple production events is discussed.

## TABLE OF CONTENTS

<u>SECTION</u>	<u>TITLE</u>	<u>PAGE</u>
I.	Foreword - - - - -	1
II.	Experimental Apparatus - - - - -	2
III.	Part 1. A $\Lambda^0$ -Fragment Decay in a Cloud Chamber	
	A. Introduction - - - - -	6
	B. Description of the Event - - - - -	9
	C. Conclusions - - - - -	11
	D. Tables and Figures to Part 1. - - - - -	14
IV.	Part 2. Associated Production of a $\Xi^-$ and Two $\theta^0$ Particles	
	A. Introduction - - - - -	23
	B. Description of the Event - - - - -	23
	C. Conclusions - - - - -	26
	D. Tables and Figures to Part 2. - - - - -	29
V.	Part 3. A Study of Multiple V-Events	
	A. Introduction - - - - -	34
	B. Geometrical Data on Double $V^0$ Decays -	37
	C. Tables and Figures to Part 3B. - - - - -	43
	D. Types of Associations Observed - - - - -	50
	E. Tables and Figures to Part 3D. - - - - -	55
VI.	References	
	A. Part 1. - - - - -	60
	B. Part 2. - - - - -	61
	C. Part 3. - - - - -	61

## FOREWARD

One of the achievements of modern cosmic ray physics has been the identification of many of the short lived particles produced in high energy nuclear interactions. Though this represents a considerable accomplishment, the problem of understanding their behavior remains. It is in the latter area that this thesis will, hopefully, make a contribution.

Within the last three years the theoretical proposals of Gell-Mann and others have brought a deeper understanding of the production and decay of unstable particles. These proposals provide the basis for the interpretation of the data of this thesis.

## EXPERIMENTAL APPARATUS

Since January 1953, the cosmic ray group at the California Institute of Technology has operated a set of cloud chambers mounted in the gap of a large electromagnet at Pasadena (220 m elevation). Much useful information obtained from this apparatus has been reported in the literature. <sup>(1)</sup>

Since this cloud chamber array has been described elsewhere, <sup>(2, 3)</sup> only a brief description will be included here. Fig. 1 shows a side view of the apparatus as it operated until July, 1953. At this time, the two top chambers were replaced by a large single chamber. All chambers were mounted in the gap of an 80 kilowatt electromagnet which produced a field of approximately 8000 gauss over the chambers.

The sensitive regions were filled with a mixture of argon gas and a vapor in equilibrium with a small puddle of liquid composed of two parts ethyl alcohol and one part water. This atmosphere was maintained at temperatures near 27°C and at pressures near 100 cm Hg.

The expansion apparatus was triggered by a conventional penetrating shower detector which consisted of three trays of eight geiger counters each mounted as shown in Fig. 1. About 50 gm/cm<sup>2</sup> of lead absorber was placed between the chambers, and 200 gm/cm<sup>2</sup> of lead was used between the top cloud chamber and the first element of the penetrating shower detector. For a period of five months, the lead between the chambers was replaced by copper.

Parallel channels using two coincidence requirements, usually 2-2-1 (two or more counts from top tray, two or more from middle tray, and one or more from bottom tray) or 0-2-2, triggered the cloud chambers.

The methods of track measurement have been described by Van Lint.<sup>(3)</sup> Errors were assigned on the assumption that 4 Bev/c was the maximum detectable momentum for tracks of 20 cm length except where there were visible distortions in the tracks, in which case a lower limit was assigned.

Caption to Figure 1

Side view of the cloud chambers, geiger counters, and absorbers.



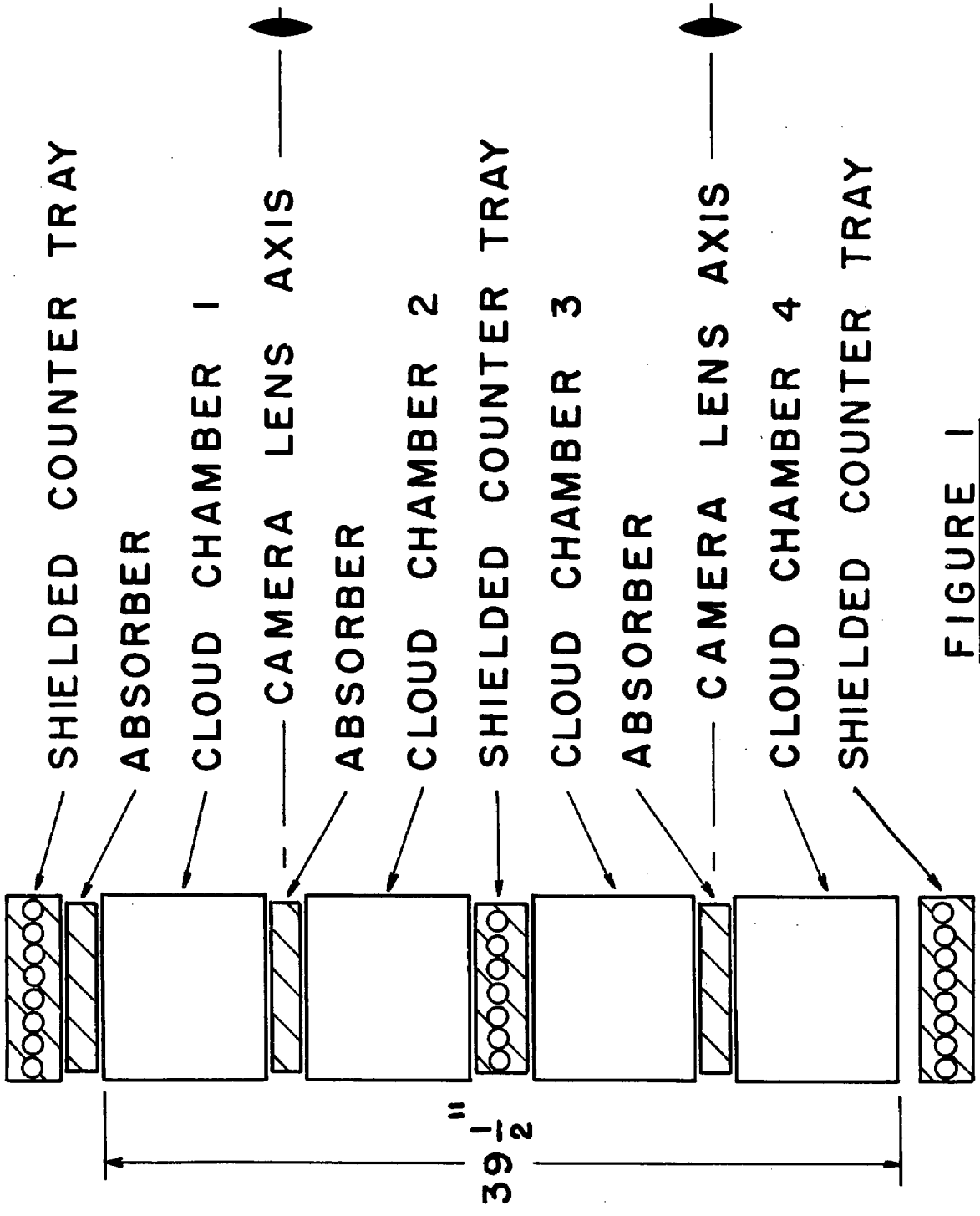


FIGURE 1

PART 1

A  $\Lambda^0$ -FRAGMENT DECAY IN A CLOUD CHAMBER

1 A. INTRODUCTION

The first discovery that a nuclear fragment could remain in an excited state long enough for a nuclear emulsion to bring it to rest was made by Danysz and Pniewski<sup>(4)</sup> at Warsaw. They observed a 21 + 18 p star (one with a charged primary, producing 21 heavily ionizing tracks and 18 lightly ionizing tracks) which ejected a 60 Mev fragment of charge about 5e. After the necessary  $3 \times 10^{-12}$  sec, the fragment stopped and subsequently decayed into another star with energy release of more than 120 Mev. No charged  $\pi$ -meson was emitted.

Danysz and Pniewski suggested that this event might be due to a nuclear fragment containing a  $\pi$ -meson in a bound orbit of long lifetime, or to the presence of an unstable hyperon which decayed after the fragment came to rest. In either situation, the fragment was supposed to have absorbed a  $\pi$ -meson and erupted with the emission of an energy nearly equal to that of the  $\pi$ -mass.

Tidman, et al.<sup>(5)</sup>, discovered a similar event shortly afterward. A 6 Bev primary created a 17 + Op star from which was ejected an excited fragment of charge 2 or 3e. After stopping, the fragment decayed with the release of more than 50 Mev. Again no charged  $\pi$ -meson was emitted, and the same interpretations were offered as for the first event. The discovery of this second event tended to remove the possibility that the first event could have been due to some freak or chance juxtaposition of tracks.

The possibility that a  $\pi$ -meson in a bound orbit could be responsible for all delayed decays of nuclear fragments was excluded by a

later event discovered by Crussard and Morellet.<sup>(6)</sup> Their event had a 30 + 30 p star with an excited fragment of charge 2 or 3e which produced a small secondary star of about  $28 \pm 4$  Mev. In this case a  $\pi$ -meson was actually emitted. The energy of decay was not large enough to be due to the absorption of a  $\pi^-$ , but the excitation of the fragment must have been large enough to produce one. Crussard and Morellet went so far as to calculate the Q-value of the  $\Lambda^0$  decay on the assumption that the binding energy of a  $\Lambda^0$ -particle is the same as for a neutron. The assumption is now known to be false, but they obtained

$$Q = 48 \pm 4 \text{ Mev for } \text{He}^{4*} \longrightarrow \text{He}^3 + p + \pi^-$$

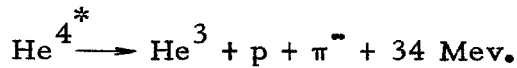
and

$$Q = 35 \pm 4 \text{ Mev for } \text{Li}^{7*} \longrightarrow \text{Li}^6 + p + \pi^-$$

Since it appears from recent results that the  $\Lambda^0$  is bound much less strongly in  $\text{He}^{4*}$  than is a neutron in ordinary  $\text{He}^4$ , the incorrect value obtained for Q in the first reaction does not indicate that the secondary star was a  $\text{Li}^7$  star. Rather, using the correct value of  $37 \pm .5$  Mev for the Q value of  $\Lambda^0$  decay,<sup>(7)</sup> we obtain a  $\Lambda^0$  binding energy of  $9 \pm 5$  Mev in fair agreement with later observations. For  $\text{Li}^7$  we get about the same  $\Lambda^0$  binding energy. Either case is possibly the one Crussard and Morellet observed.

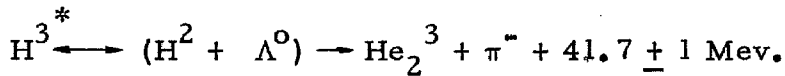
Following the discovery of other confirmatory examples,<sup>(8, 9)</sup> Hill<sup>(10)</sup> and associates at Brookhaven observed an event which is subject to more precise analysis than any event previously reported. The mass of the ejected fragment was measured and found consistent

with  $\text{He}^3$ . Their interpretation is



Thus the first good measure of the binding energy of the  $\Lambda^0$  in an identified nucleus was obtained.

Both delayed mesonic and non-mesonic decay were then well established. Moreover, a new interesting event of Bonetti, et al.,<sup>(11)</sup> showed non-protonic decay! The interpretation of their event is

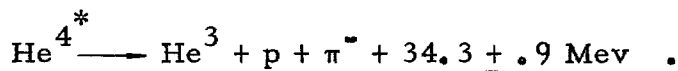


Consideration of the masses of  $\text{H}^3$  and  $\text{H}^2 + \Lambda^0$  gives a  $\Lambda^0$  binding energy in  $\text{H}^{3*}$  of  $.7 \pm 2$  Mev.

The cases of Hill and Bonetti give the best measures of binding energy of the  $\Lambda^0$  available.

Many other examples of delayed fragment decays interpreted as  $\Lambda^0$ -fragment events have been reported.<sup>(12 - 17)</sup>

A K-meson becomes involved in the subject of delayed fragments in the case of Naugle, et al.<sup>(18)</sup> In this case a stopping K-meson of measured mass  $1010 \pm 200 m_e$  makes a  $50 \pm 8$  Mev star. One of the ejected prongs is believed to be an excited  $\alpha$ -particle which probably undergoes the decay seen at Brookhaven,



The binding energy of the  $\Lambda^0$  becomes  $2.8 \pm 1.4$  Mev. The charge of the fragment is not certain.

From the above examples, the nuclear emulsion experimenters have firmly established the existence of  $\Lambda^0$ -fragments of short range

and lifetime  $> 10^{-12}$  sec.

Some anomalous cases of long lived fragments have been observed that cannot be explained by the assumption of a bound  $\Lambda^0$ , but these events are very rare indeed. (19, 20)

## 1 B. DESCRIPTION OF THE EVENT

In the 48-inch magnet cloud chambers, the event shown in Fig. 2 has been observed. This photograph contains what appears to be the decay of an ordinary  $\Lambda^0$  into a proton (track B) and a  $\pi^-$  meson (track C). The momenta, estimated ionizations, and derived masses of the labelled tracks are shown in Table I. The ionization and momentum of track B determine that it is probably due to a proton (mass =  $1850 \pm 350 m_e$ ), while track C could not be due to a particle as heavy as known K mesons. It is, however, consistent with either a  $\pi$ -meson,  $\mu$ -meson, or electron.

If we assume that C is the track of a  $\pi^-$  meson, B and C together have the usual characteristics of  $\Lambda^0$  decay. The measured Q value is  $36.6 \pm 2.9$  Mev, in good agreement with the known value of  $37.0 \pm .5$  Mev.

However, there are several unusual characteristics of this event which raise doubt that it is in fact an ordinary  $\Lambda^0$  decay.

1. The only penetrating shower origin associated with this event is 5 mm above the top inside wall of the cloud chamber. Even though all tracks of more than 300 Mev/c momentum pass through this origin, it does not lie in the  $\Lambda^0$  decay plane. The angle of non-coplanarity is  $4.1 \pm 2.0^\circ$ .

2. The line of flight of the  $\Lambda^0$  determined from the momentum of the decay products misses this origin by  $7 \pm 2$  mm.

3. The vertex of the assumed  $\Lambda^0$  lies on the path of a heavy fragment (track A) ejected from the penetrating shower origin, within an experimental error of .1 mm laterally and .4 mm in depth.

4. There is a  $3.0 \pm 1.2^\circ$  kink in the fragment track where it meets the vertex of the assumed  $\Lambda^0$ , whereas none of the shower tracks in the photograph shows detectable distortion.

5. The direction and magnitude of this kink are such that transverse momentum balance is possible if we assume that the fragment A undergoes a decay into B, C, and D. Table II gives the rectangular components of unit vectors oriented along the tangents to the tracks A, B, C, and D at their intersection, with respect to axes  $X'$ ,  $Y'$ ,  $Z'$  such that track A is travelling in the negative  $Y'$  direction. Figures 3, 4, and 5 show an isometric view of the four tracks; the intersection points of the tangents to tracks B, C, and D with a plane perpendicular to track A; and a transverse momentum diagram, respectively. Transverse momentum balance is excellent for a doubly charged fragment, but it is barely within experimental error for a singly charged one.

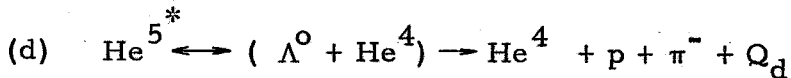
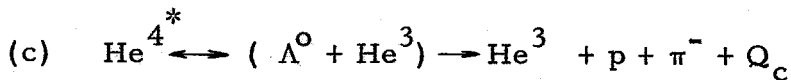
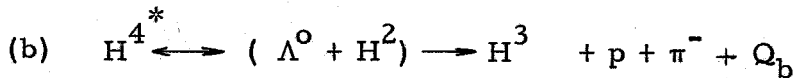
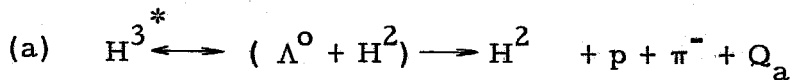
The above characteristics strongly suggest that this event is an example of the decay of a  $\Lambda^0$  particle bound to a nuclear fragment, and therefore a detailed analysis based upon this assumption has been carried out.

By comparison with the ionization of protons of known momenta, the ionization of the fragment below the kink is estimated to be within

the range 15 to 30 times minimum. In Table III, the measured momenta, with errors including those due to multiple scattering, and required ionizations are listed opposite the various possible secondary fragment identities. We see that the secondary fragment is probably either  $H^3$  or  $He^3$ , but there is a small possibility that it is  $H^2$  or  $He^4$ .

### 1 C. CONCLUSIONS

If this event is an example of a  $\Lambda^0$ -fragment decay, the possible identities of the secondary fragment require that it be one of the following types:



The Q values that correspond to these possibilities are:

$$Q_a = 42.8 \begin{matrix} + 4.3 \\ - 3.8 \end{matrix} \text{ Mev}$$

$$Q_b = 53.4 \begin{matrix} + 6.6 \\ - 6.2 \end{matrix} \text{ Mev}$$

$$Q_c = 38.9 \begin{matrix} + 3.7 \\ - 3.4 \end{matrix} \text{ Mev}$$

$$Q_d = 44.0 \begin{matrix} + 5.7 \\ - 4.6 \end{matrix} \text{ Mev}$$

If the proton and  $\pi$ -meson are regarded as the decay products of a

$\Lambda^0$  particle residing in the fragment, we may derive the binding energy of the  $\Lambda^0$  within the fragment by subtracting the above Q values

from the 37.0 Mev  $Q$  value of  $\Lambda^0$  decay. We thus obtain the  $\Lambda^0$  binding energies ( $q$ ), for the four possibilities:

$$q_a = \begin{array}{r} -5.9 + 3.8 \\ -4.3 \end{array} \text{ Mev}$$

$$q_b = \begin{array}{r} -16.4 + 6.2 \\ -6.6 \end{array} \text{ Mev}$$

$$q_c = \begin{array}{r} -1.9 + 3.4 \\ -3.7 \end{array} \text{ Mev}$$

$$q_d = \begin{array}{r} -7.0 + 4.6 \\ -5.7 \end{array} \text{ Mev}$$

Only in case (c) could the  $\Lambda^0$  have a positive binding energy within the stated errors of measurement.

If we should assume that neutrons are among the secondaries, the binding energy would, of course, be even smaller. Since momentum balance is possible without assuming neutral secondaries, we conclude that the decay is probably of type (c), and the binding energy of the  $\Lambda^0$  to  $\text{He}^3$  is probably less than 2 Mev.

This event is unique in two respects. In the first place, it has a high fragment momentum, which is  $1600 \pm 300$  Mev/c when extrapolated back to the origin of the penetrating shower. In nuclear emulsion events, the excited fragments observed have had ranges that correspond to much smaller momenta. It is conceivable that this may be due to a strong bias in the method of detecting the events. In nuclear emulsions, the  $\Lambda^0$ -fragments are detected by scanning for two stars close together and connected by a heavily ionizing track. An event similar to the one presented here would not have been observed at all in most emulsion stacks because the excited fragment would have emerged before decay. In some of the largest emulsion blocks used, a 1600 Mev/c  $\text{He}^{4*}$  nucleus might stop, but the search



for such an event would be very laborious due to the large separation between connected stars.

Secondly, this is the only case where the time of flight before decay can be measured. Previously it has been possible to set only a lower limit to the lifetime because all fragments stopped in emulsion before decay. If our interpretation is correct, the lifetime of the excited  $\text{He}^4$  was  $5.4 \pm .6 \times 10^{-10}$  sec for this single example. This figure is of the order of the free  $\Lambda^0$  lifetime,  $3.7 \pm 10^{-10}$  sec. Therefore, the induced decay of a  $\Lambda^0$  due to the presence of nuclear matter is not a strong effect. This result is consistent with the Gell-Mann scheme of unstable particles, for there is no lighter system of the same strangeness into which the bound  $\Lambda^0$  might decay through a rapid exothermic reaction (see Fig. 9, Part 3).

Fry has observed only about one such delayed fragment decay per 1000 emulsion stars. <sup>(19)</sup> If we assume that this is a reasonable figure for the frequency of occurrence of  $\Lambda^0$ -fragments in penetrating showers, we would expect that only 10 such fragments were produced by the 10,000 penetrating showers recorded by the 48-inch apparatus. For one such fragment to be observed, the shower would have to a) occur within approximately the last  $10 \text{ gm/cm}^2$  of absorber above a chamber, b) occur well away from the cloud chamber walls, c) take place when cloud chamber distortions are a minimum, d) surround the fragment with a few but not too many comparison tracks, e) and project a fragment into the cloud chamber with velocity such that the fragment decay would occur in the visible part of the chamber. Cloud chamber examples of delayed fragment decays will probably remain rare.

Table I. Basic data on tracks of Fig. 1.

Track	Charge	Momentum Mev/c	Ionization Times minimum	Mass $m_e$
A	—	—	15 - 30	—
B	+	$298 \pm 31$	5 - 10	$1850 \pm 350$
C	-	$145.5 \pm 6$	$< 2$	$< 370$
D	+	See Table III	15 - 30	—

Table II. Rectangular components of unit vectors.

Particle Identification	Designation of Tangents in Fig. 2	Unit Vectors of Tangents <sup>a</sup> at Decay Point
Fragment before decay	O'A (or O'A')	$(.000 + .012) i + (1.000) j + (.000 + .024) k$
Proton	AB	$-.3330 i - .9238 j - .1889 k$
$\pi$ -Meson	AC	$+.4808 i - .8726 j + .0867 k$
Fragment after decay	AD	$+.1212 i - .9986 j + .0486 k$

a. The errors in measurement of the direction cosines of AB, AC, and AD are negligible in the analysis of this event.

Table III. The required ionization corresponding to various assumptions for the secondary fragment (Track D, Fig. 2). The ionization of the secondary fragment is estimated to be between 15 and 30 times minimum.

Assumed Secondary Fragment	Corresponding Momentum Mev/c	Required Ionization Times Minimum	Interpretation Based on Ionization Estimates
H <sup>1</sup>	445 + 62	3.4 - 4.8	Excluded
H <sup>2</sup>	445 + 69	9.2 - 15	Unlikely
H <sup>3</sup>	445 + 81	17 - 28	Possible
He <sup>3</sup>	890 + 131	21 - 41	Possible
He <sup>4</sup>	890 + 138	37 - 62	Unlikely
Li <sup>6</sup>	1335 + 207	56 - 93	Excluded

Captions to Figures of Part 1

- Fig. 2. A cloud chamber photograph of a delayed fragment decay. A heavy fragment (A) is ejected from a well defined shower origin 5 mm above the sensitive region of the chamber. The fragment subsequently decays into a proton (B), a light particle consistent with a  $\pi^-$  meson (C), and another secondary fragment (D). The event is consistent with the in flight decay of an excited  $\text{He}^4$  nucleus containing a  $\Lambda^0$  particle. An unrelated  $\pi \rightarrow \mu + \nu$  decay appears slightly to the left of track (D).
- Fig. 3. An isometric view of the event shown in Fig. 1. The penetrating shower has a neutral primary for there is no track visible in the chamber above the one shown. The lines of this figure are all tangents to the pertinent tracks at the decay point (A) of the excited fragment. Thus O'A, the tangent to the primary fragment, does not pass exactly through O, the origin of the penetrating shower. AA' is a straight line extension of O'A. Orthogonal projections of the event are drawn on the back piston and a side wall.
- Fig. 4. The intersections of the lines of flight of the tracks of Fig. 2 with a plane transverse to the line of flight of the primary fragment. This figure shows that the sum of the transverse momenta of the proton and  $\pi^-$  meson is opposite in direction to the transverse momentum of the secondary fragment, within experimental error. The ellipse around the origin of the diagram represents the error in measurement of the

tangent to the primary fragment at the point of decay. The errors in measurement of the directions of the secondary fragment, proton, and  $\pi$ -meson are negligible compared to that of the primary fragment. The large circle on the diagram represents the locus of intersections made by lines which pass through Point A, Fig. 2, and make an angle of  $10^\circ$  to the  $Y'$  axis.

Fig. 5. Transverse momenta of the secondaries of the  $\Lambda^0$ -fragment decay. One region of error is drawn for the vector sum of the transverse momenta of the proton and  $\pi$ -meson. Two other regions of error are drawn for the secondary fragment, one for a doubly charged fragment and another for a singly charged fragment. Momentum balance is excellent for the case of a doubly charged fragment.

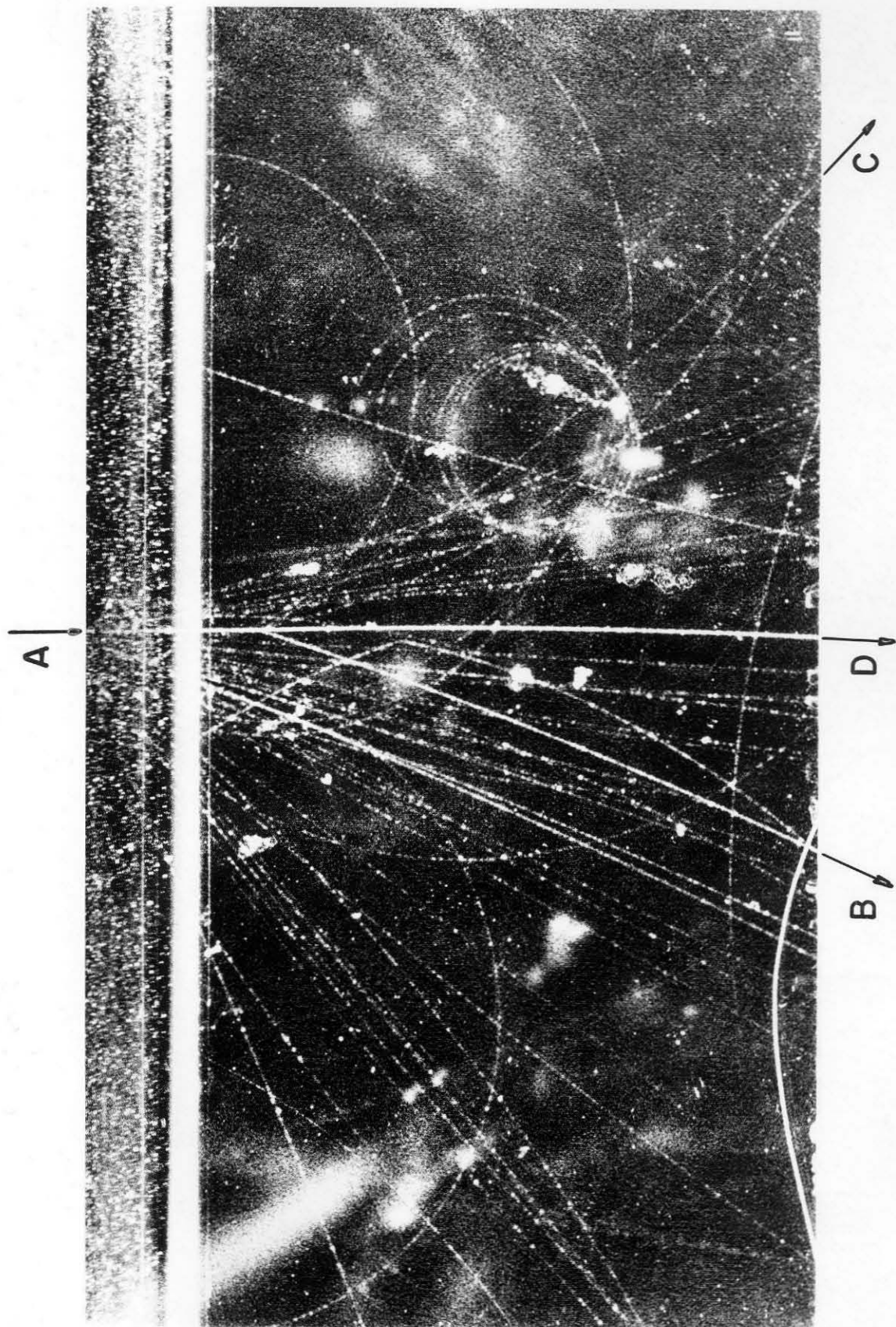


FIGURE 2

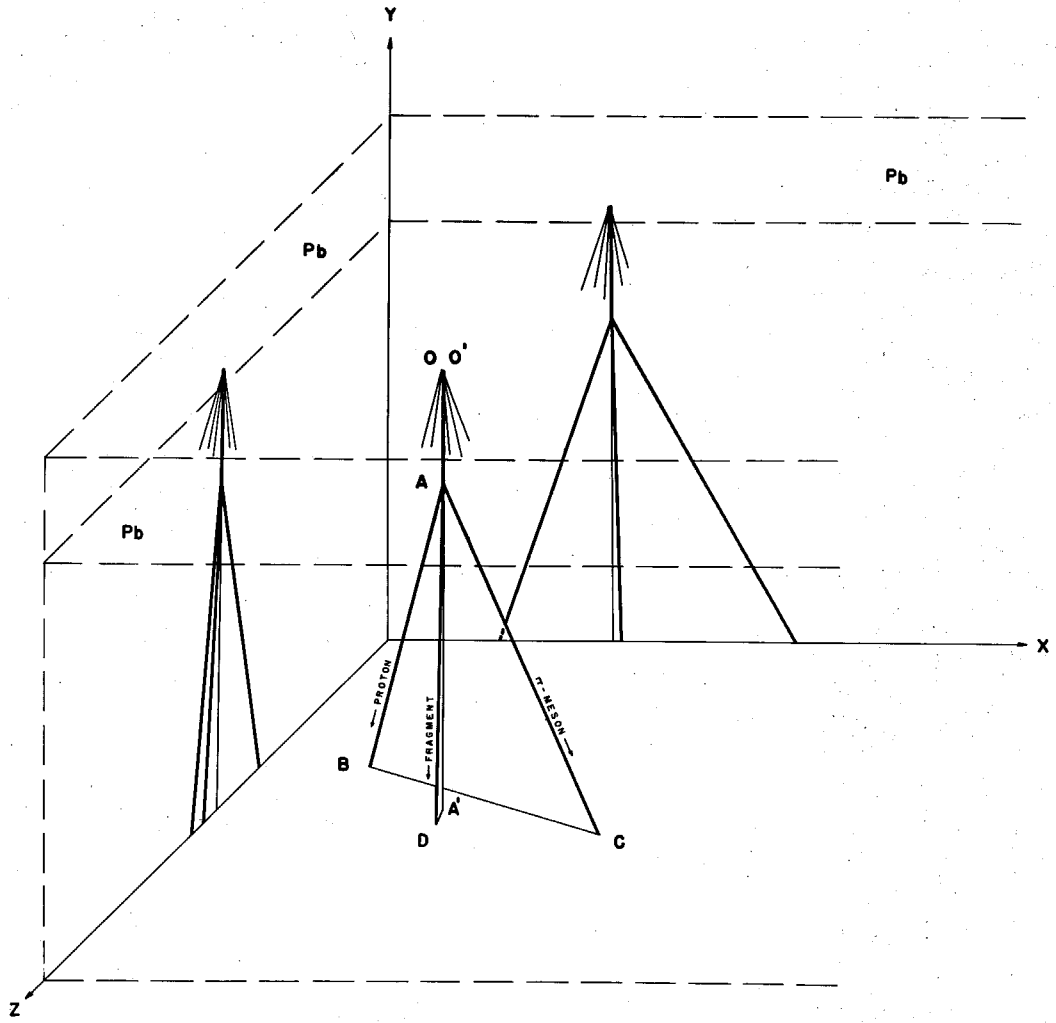


FIGURE 3



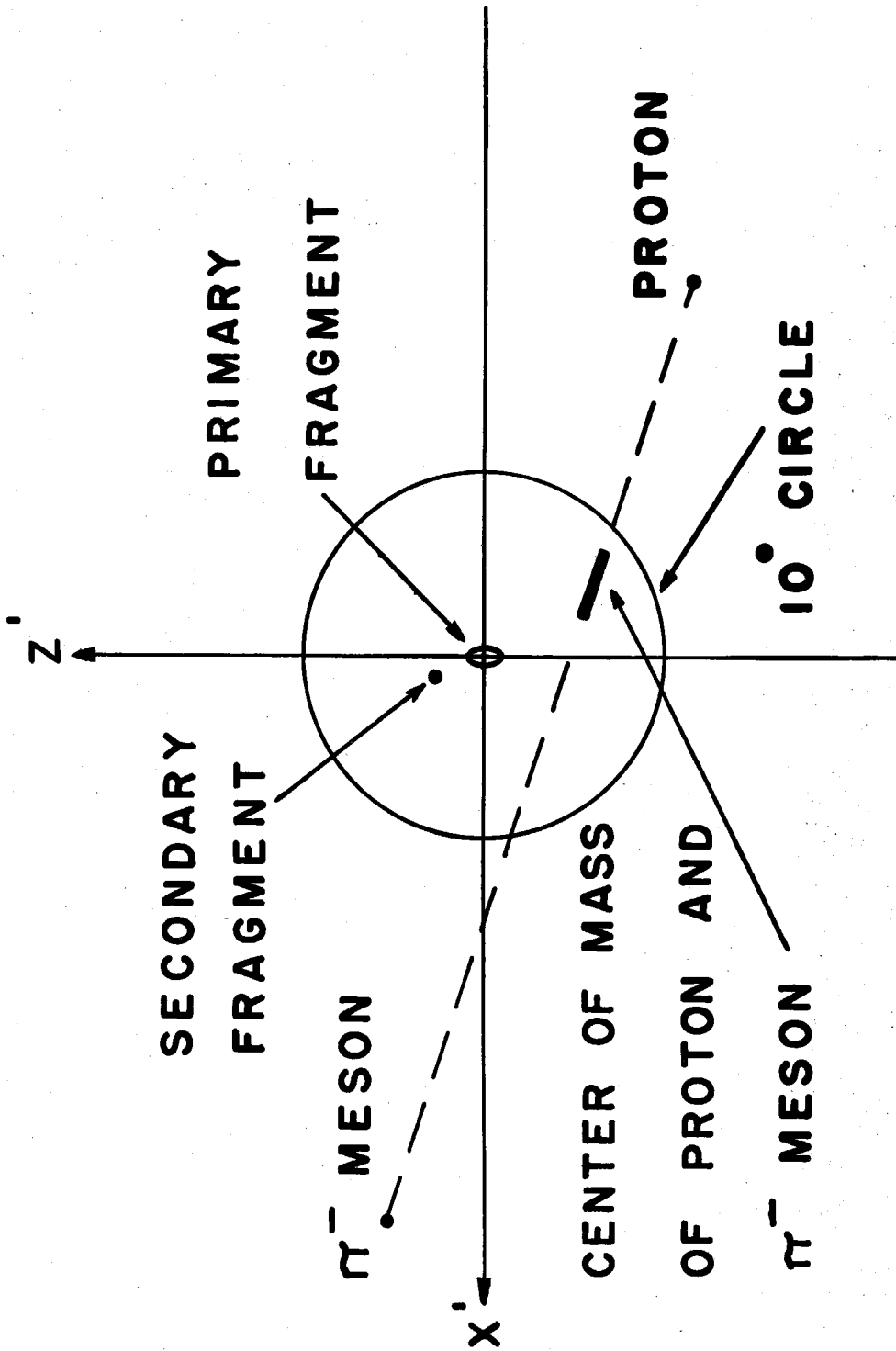


FIGURE 4

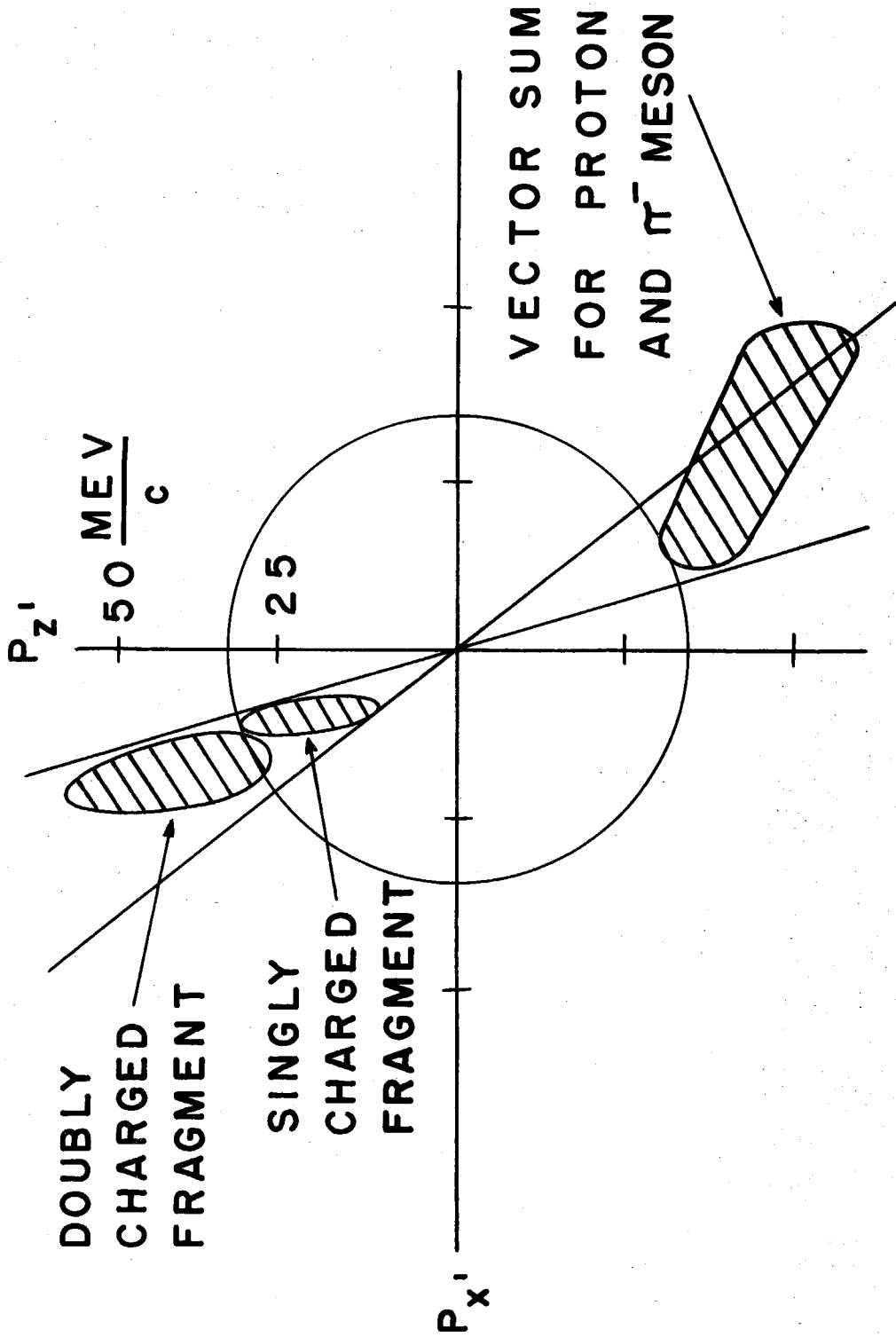


FIGURE 5

PART 2

EXAMPLE OF THE ASSOCIATED PRODUCTION OF A  $\Xi^-$   
AND TWO  $\theta^0$  PARTICLES

2 A. INTRODUCTION

In another extraordinary photograph (Fig. 6) obtained from the 48-inch magnet cloud chambers, four V-events appear in the same penetrating shower. Since this shower originated just above the sensitive region of the chamber, and it is unaccompanied by any other nearby nuclear interactions, the location of the origin can be precisely determined. Because of this fortunate circumstance, the analysis of the four V-events can be carried out in some detail with a very interesting result.

2 B. DESCRIPTION OF THE EVENT

An isolated primary particle of  $>4$  Bev/c momentum and unknown sign of charge enters from above and behind chamber 2, Fig. 1. Only 6 mm above the top inside wall of chamber 3, the primary makes a high energy nuclear interaction which produces the penetrating shower containing the four V-particles, all of which decay in chamber 3. There are no other tracks besides the primary in chambers 1 and 2, and all of the tracks in chambers 3 and 4 appear to result from the single interaction at the top of chamber 3.

In Fig. 8, the various decays are shown in an isometric projection of the tangents to the pertinent tracks at their decay points. All decay secondaries pass through the front of the apparatus except for FH and IK which travel down through chamber 4.

There are three  $V^0$  decays, FGH, CDE, and IJK. The planes

of both FGH and IJK pass through the origin O within experimental error, the angles of noncoplanarity for O with respect to FGH and IJK being  $2.8 \pm 4^\circ$  and  $.5 \pm 1.4^\circ$  respectively. Moreover, the lines of flight of the corresponding  $V^0$  particles computed from measured momenta and assuming two body decay also pass through O within experimental error.

However, plane CDE does not contain O, the angle of noncoplanarity being  $7.8 \pm 1.5^\circ$ . Instead, the plane of CDE contains the decay point A of a  $V^-$  event, OAB, the measured angle of noncoplanarity being  $.2 \pm 1.3^\circ$ .

Information concerning the tracks pertinent to the interpretation of this event are given in Tables IV and V. Momenta for FH and IK in chamber 3 were determined from curvature measurements in chamber 4 with correction for the lead absorber and brass chamber walls in between.

Both FGH and IJK must have light positive secondaries to be consistent with their estimated ionizations and measured momenta. Independently of any ionization estimates, the  $a$  and  $P \sin \theta_T$  values exclude the possibility that FGH and IJK might be  $\Lambda^0$  decays. Under the assumption of the decay

$$\theta^0 \rightarrow \pi^+ + \pi^- + Q(\pi, \pi)$$

FGH gives

$$Q(\pi, \pi) = 240 \pm 60 \text{ Mev}$$

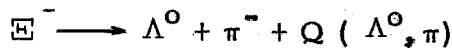
from the measured momenta of the secondaries. The momentum of the positive secondary of IJK cannot be determined directly, but by assuming two body decay and momentum balance we obtain from the

momentum of the negative secondary

$$Q(\pi, \pi) = 270 \pm 70 \text{ Mev} .$$

Therefore, FGH and IJK are quite consistent with normal  $\theta^0$  decay where  $Q(\pi, \pi) = 214 \text{ Mev}$ .

The third  $V^0$  decay, CDE, cannot be identified directly from the characteristics of its secondary tracks. However, the established coplanarity of this decay plane with the decay point of the  $V^0$  particle suggests strongly that it is the secondary of the well known  $\Xi^-$  decay,

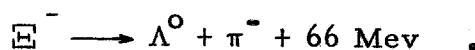


and is thus a  $\Lambda^0$  particle. The  $Q(\Lambda^0, \pi)$  for the assumed  $\Xi^-$  decay can be computed from the roughly measured momentum of the negative secondary, AB, and the geometry of the event. The result is

$$Q(\Lambda^0, \pi) = 95 \begin{matrix} +100 \\ -50 \end{matrix} \text{ Mev}$$

which is consistent with previously measured values<sup>(21)</sup> of  $\sim 66 \text{ Mev}$ .

The momentum of the assumed  $\Lambda^0$  can be obtained from transverse momentum balance with AB, but a more precise value can be obtained from the geometry of the  $\Xi^-$  decay if we assume the decay scheme



From the derived momentum of the  $\Lambda^0$  ( $792 \pm 50 \text{ Mev}$ ) and its decay geometry, we obtain for

$$\Lambda^0 \rightarrow P + \pi^- + Q(p, \pi)$$

a  $Q(p, \pi)$  value of  $32 \pm 10$  Mev in agreement with the known value of 37 Mev. Conversely, if we assume that CDE is indeed a 37 Mev  $\Lambda^0$  decay, we may calculate the momentum of the  $\Lambda^0$  from geometrical factors only. From this new  $\Lambda^0$  momentum and the geometry of the  $E^-$  event, we obtain

$$Q(\Lambda^0, \pi) = 76 \pm 15 \text{ Mev} ,$$

in good agreement with the known value. Therefore, the decay dynamics are completely consistent with the interpretation that CDE is the secondary  $\Lambda^0$  of a  $E^-$  event OAB.

## 2 C. CONCLUSIONS

Since there is evidence of only one nuclear interaction which could produce these unstable particles, it appears that the  $E^-$  was very probably produced in association with two  $\theta^0$  particles. Such a process is in direct agreement with the ideas presented by Gell-Mann. (22)

TABLE IV. Basic Data

Track	Charge	Measured momentum Mev/c	Estimated ionization times minimum	Estimated mass from ionization vs. momentum in $m_e$	Best direction cosines <sup>b</sup>
				l	m n
PO	?	> 4000	< 2	—	-.0625 -.9591 +.2764
OA	-	> 200	< 2	—	-.0756 -.9579 +.2773
OF	0	—	—	—	-.3889 -.9160 +.0994
OI	0	—	—	—	-.0211 -.9612 +.2748
AB	-	500 <sup>+500</sup> -250	< 2	< 2000	+ .1489 -.9165 +.3714
AC	0	—	—	—	-.1380 -.9680 +.2091
CD	-	> 180	< 2	—	-.2222 -.8716 +.4368
CE	+	> 180	< 2	—	-.1116 -.9855 +.1282
FG	+	520+150	< 2	< 1500	-.5056 -.7684 +.3924
FH	-	920+220 <sup>a</sup>	< 2	< 2800	-.1992 -.9759 -.0895
IJ	-	> 640	< 2	—	+ .0671 -.9083 +.4131
IK	+	475+110 <sup>a</sup>	< 2	< 1350	-.2139 -.9696 -.1190

a. These are values determined for chamber 3 from curvature measurements in chamber 4 with correction for the lead and brass in between.

b. Errors in measurement of direction cosines are  $\pm .015$  or less for all l and  $\pm .04$  or less for all n.

Caption for TABLE V

TABLE V. Numerical results for the decays of Fig. 3. The values for  $\alpha_a$  are computed for the four V-particle decays, ABC, CDE, FGH, and IJK from angles only. The values for  $\alpha_p$  are computed from momentum measurements alone. The angle  $\theta_T$  is the total included angle between decay secondaries. The values of  $P \sin \theta_T$  listed in the fourth column must be less than 118 Mev/c for  $\Lambda^0$  decay, which is not the case for FGH and IJK. ABC and CDE appear to be members of a cascade event and are therefore interpreted as  $E^-$  and  $\Lambda^0$  decays respectively. The noncoplanarity angles,  $\delta$ , with assumed origins are all zero within experimental error. The Q value for FGH was obtained from  $\theta_T$  and the momenta of the secondaries. The Q values in column 7 for both ABC and IJK were obtained from  $\theta_T$ , the momentum of one measurable secondary in each case, and the transverse momentum about their lines of flight. The Q values in column 8 were obtained from the cascade relationship between ABC and CDE as described in the text.



TABLE V. (Caption on previous page)

Decay Plane	$1^a$	$2^b$	$3$ $\theta_T$ degrees	$4$ $P \sin \theta_T$ Mev/c	$5$ Interpretation	$6$ $\delta$ Noncoplanarity angle degrees	$7$ Q Values From Mo- menta and Geom. Mev	$8$ Q Values From case and geom. Mev
ABC	$+5 \pm 1$	—	$19.2 \pm 1$	$160^{+160}_{-80}$	$E^-$ decay	—	$95^{+100}_{-50}$	$76 \pm 15$
CDE	$+5 \pm 3$	—	$20.0 \pm 2$	$> 61$	$\Lambda^0$ decay	$.2 \pm 1.0$	—	$32 \pm 10$
FGH	$-.13 \pm .05$	$-.29 \pm .26$	$35.4 \pm 1$	$535 \pm 125$	$\theta^0$ decay	$2.8 \pm 4$	$240 \pm 60$	—
IJK	$-.46 \pm .08$	$-.05$	$35.2 \pm 2$	$> 370$	$\theta^0$ decay	$.5 \pm 1.4$	$270 \pm 70$	—

a.  $\alpha_a = \frac{\sin(\theta_- - \theta_0)}{\sin(\theta_- + \theta_0)}$  for ABC, and  $\alpha_a = \frac{\sin(\theta_- - \theta_+)}{\sin(\theta_- + \theta_+)}$  for CDE, FGH, and IJK.

b.  $\alpha_p = \frac{P_+^2 - P_-^2}{P_0^2}$

Captions to Figures of Part 2

Fig. 6. Cloud chamber photograph of a penetrating shower which includes two  $\theta^0$  decays (FG-FH and IJ-IK), and one  $\Xi^-$  decay (OAB) with its secondary  $\Lambda^0$  (CD-CE).

Fig. 7. Enlargement of chamber 3, Fig. 6.

Fig. 8. An isometric view of the event in Fig. 7. All lines except PO are tangents to the tracks at the decay points. There is no detectable curvature in PO or OA. The primary PO makes a nuclear interaction at O, the origin of the penetrating shower which produces four V events. Decays FGH and IJK are identified as  $\theta^0$  decays from data in Tables IV and V. Point O is coplanar with both  $\theta^0$  decay planes within experimental error. However, plane CDE passes through A but not O, within errors of measurement. Thus OAB-CDE is interpreted as a cascade event. Other data summarized in the text and Tables IV and V are consistent with the interpretation that CDE is the secondary  $\Lambda^0$  of a  $\Xi^-$  event OAB. Tracks FH and IK penetrate through another cloud chamber (No. 4, Fig. 1) below the one shown in the figure.

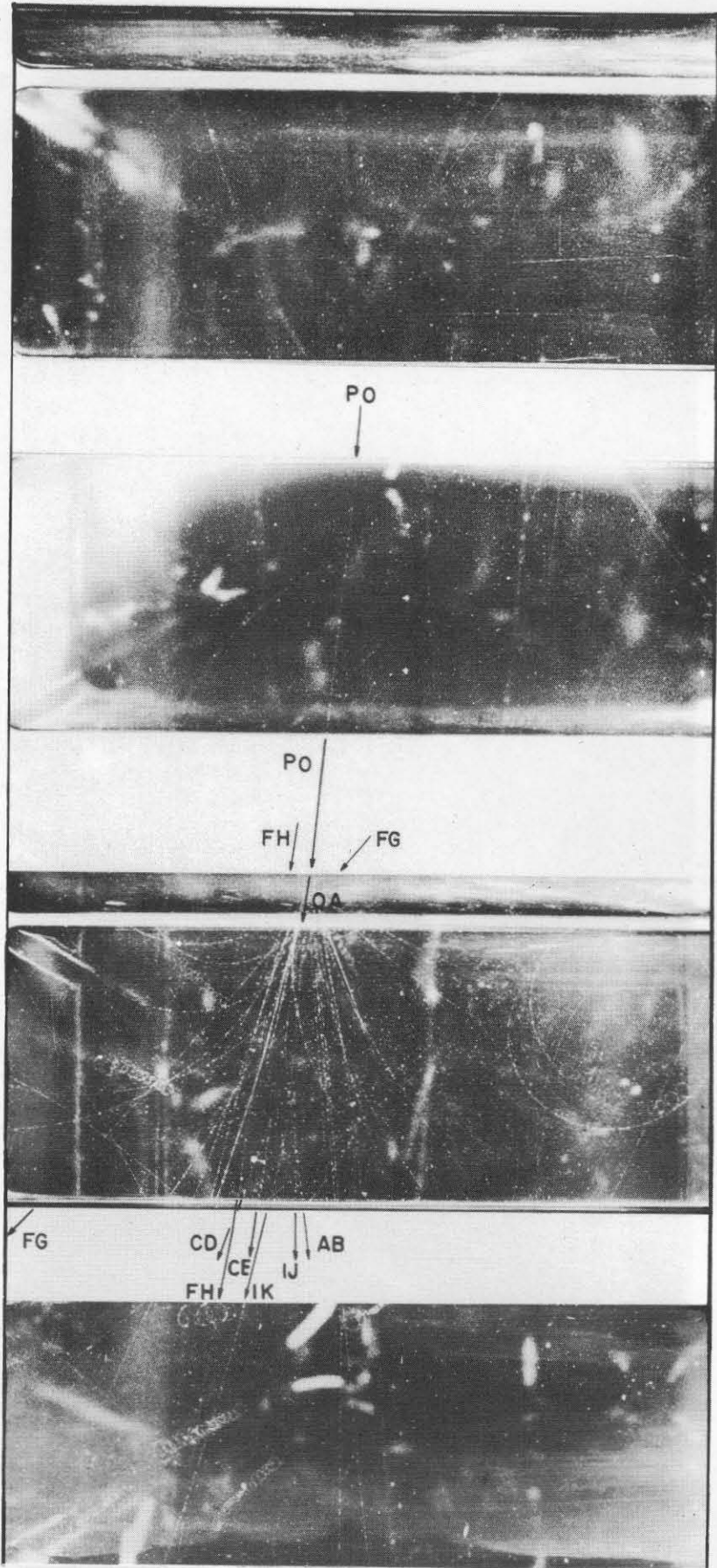
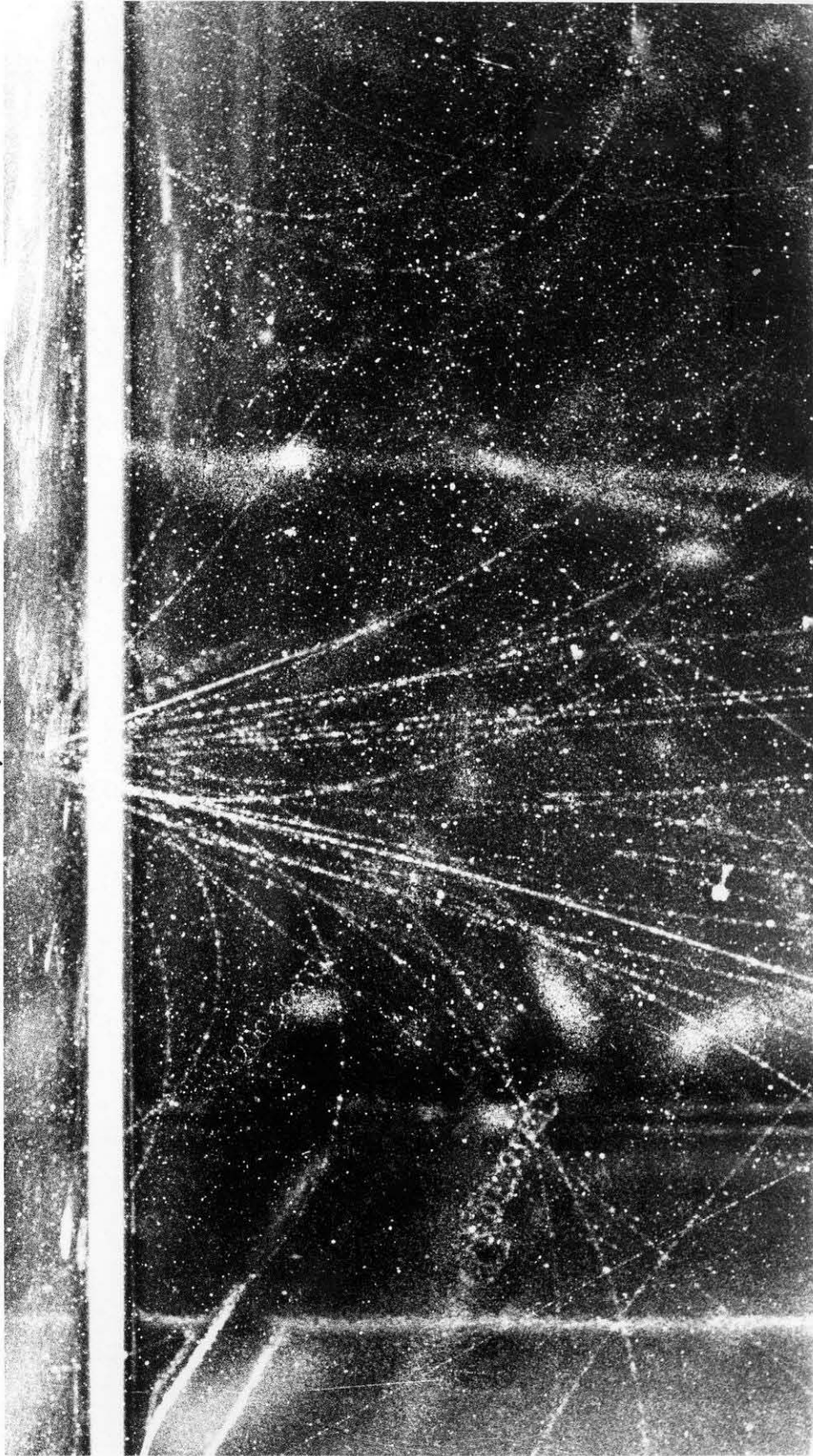


FIGURE 6

FH / OA / FG



CD / CE / IJ / AB  
FH / IK

FG

FIGURE 7

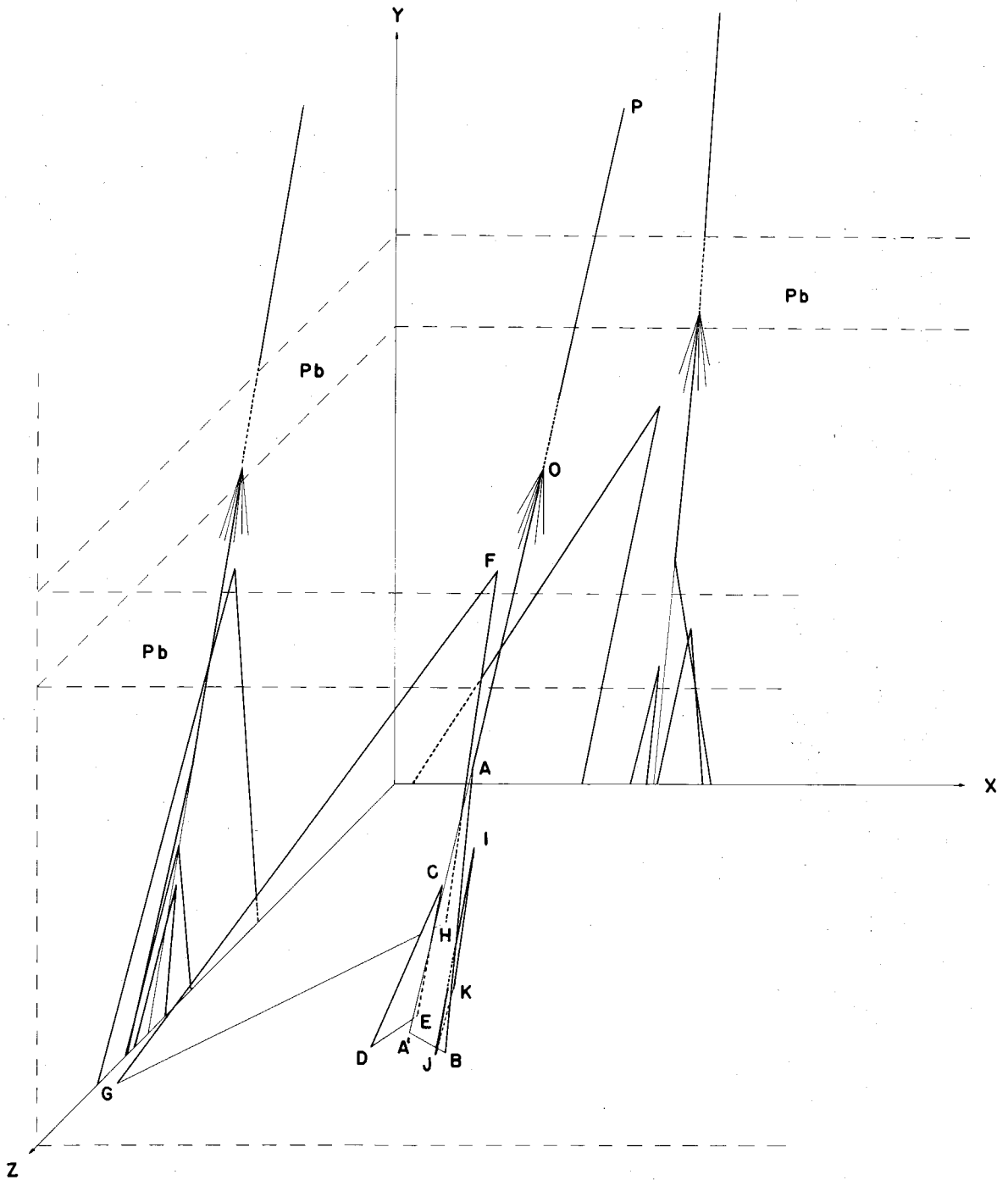


**FIGURE 8**

PART 3

A STUDY OF MULTIPLE V-EVENTS

3 A. INTRODUCTION

Within three years after the discovery of V-particles by Rochester and Butler<sup>(23)</sup> in 1947, there was evidence that

- a) the V-particles are produced copiously with a rate of greater than .01 per penetrating shower; and
- b) their lifetimes are of the order of  $10^{-10}$  sec.

These results have been confirmed by a mass of recent data.<sup>(24)</sup>

Since the production of these particles takes place in a time roughly equal to the range of nuclear forces ( $10^{-13}$  cm) divided by the speed of light ( $3 \times 10^{10}$  cm/sec), or about  $10^{-23}$  sec, we would expect from detailed balance that the lifetimes for decay would be similarly short. The observed lifetimes of about  $10^{-10}$  sec are many orders of magnitude longer.

There have been two proposals for the resolution of this apparent contradiction. One assumes that the production cross-sections are strongly dependent on energy, being very small at low energies and large at high energies. The copious production then would be due to the high energy available in a penetrating shower, and the long lifetime would be due to the small Q value of the decay.

A physical model for this condition has been proposed by Fermi and Feynman<sup>(25)</sup>. They postulate that a high centrifugal barrier inhibits the decay, but at production energies, the barrier is easily overcome. Under this model, the spin required is of the order of  $J = \frac{13}{2}$  for the  $\Lambda^0$ .

Some of the consequences of this theory are:

1. The  $E^-$  particle must have an even larger spin than its secondary  $\Lambda^0$ . If it had nearly the same, its usual decay to a  $\Lambda^0$  and  $\pi^-$  would be fast. If it had a smaller spin, its decay to a neutron and  $\pi^-$  would be fast.

2. At energies near threshold, the associated production of particles with opposite and nearly equal spin might be favored. In this event, there would be strong angular correlations among the decay products of the produced particles.

3. At energies well above threshold, single production would have large cross-section.

The other proposal which makes compatible copious production with slow decay assumes that different processes are involved in the two phenomena. In the strong production interaction two or more new particles would be created in "associated production." The decays would take place individually through an entirely different and slow process.

This solution is due originally to Nambu<sup>(26)</sup>, et al., in 1951. However, experiments in cosmic radiation shortly thereafter did not seem to indicate that associated production is the general rule. This situation obtained until the work of Shutt and collaborators at Brookhaven.<sup>(27)</sup> Using a hydrogen diffusion chamber in the 1.37 Bev  $\pi^-$  beam, these researchers found that neutral or charged hyperons can be produced with neutral or charged K-mesons.

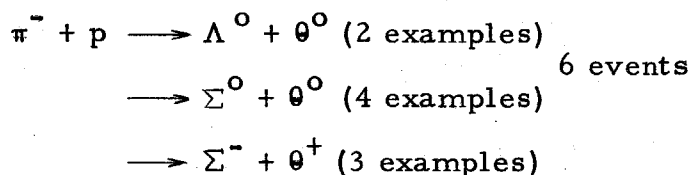
Recent data has shown that associated production occurs to some extent in cloud chambers triggered on penetrating showers<sup>(28)</sup>

and in nuclear emulsions exposed to cosmic rays.<sup>(29)</sup> Here again the evidence is that hyperons are produced associated with heavy mesons.

Gell-Mann<sup>(22)</sup> and Nishijima<sup>(35)</sup> have proposed a very economical model based on associated production which fits the data at Brookhaven very well. The particles contained in their scheme are shown as "mass levels" in Fig. 9. The particle multiplets are listed in columns according to assigned "strangeness" numbers (S).

According to the rules of this scheme,  $\Delta S = 0$  in production events and  $\Delta S = \underline{+ 1}$  in slow decay.

Researchers at Brookhaven have obtained examples of production compatible with these rules. They have seen:



where the bosons (B) observed are  $\theta^0$  and  $\theta^+$ . Their observations did not determine by themselves whether the apparent associated production occurs because of special selection rules or because of high spin of the hyperons and K-mesons, since the energies were not much above threshold.

At the time of Brookhaven's experiments there had been little evidence for associated production in cosmic ray experiments. However, the event described in Part 2 and the examples to be described later suggest that there is more associated production in cosmic rays than heretofore realized.



It is proposed by the high angular momentum theory that certain angular correlations may exist in associated production of  $V^0$  due to a large spin of the produced particles. Researchers at Princeton<sup>(30)</sup> report that angular correlations exist between the decay planes of the two  $V^0$  particles and the plane containing their lines of flight before decay. Since the normal to the planes containing the lines of flight of the  $V^0$  particles is independent of the orientation of either decay plane for a decay isotropic in the center of mass system, the existence of some correlation between planes would indicate that at least one type of  $V^0$  has a spin greater than zero<sup>(31)</sup>, and that associated production does occur. A uniform distribution of angles between decay planes and production planes does not rule out high spins, for they may be randomly oriented with respect to the plane containing the lines of flight of the V-particles. Treiman, et al., found that in 10 events the angles between decay planes and production planes showed the following relationship: when one angle was small, the other was large. Because of their small sample, a similar geometrical analysis of the CalTech data has been carried out.

### 3 B. GEOMETRICAL DATA ON DOUBLE $V^0$ DECAYS

In approximately 40,000 photographs taken of the 48-inch magnet cloud chambers, 20 events have been found where two or more neutral V-particles appear in a single chamber. No special program has been devised for the efficient selections of double  $V^0$  events, but the routine scanning of all photographs for interesting single events has produced these 20 cases.

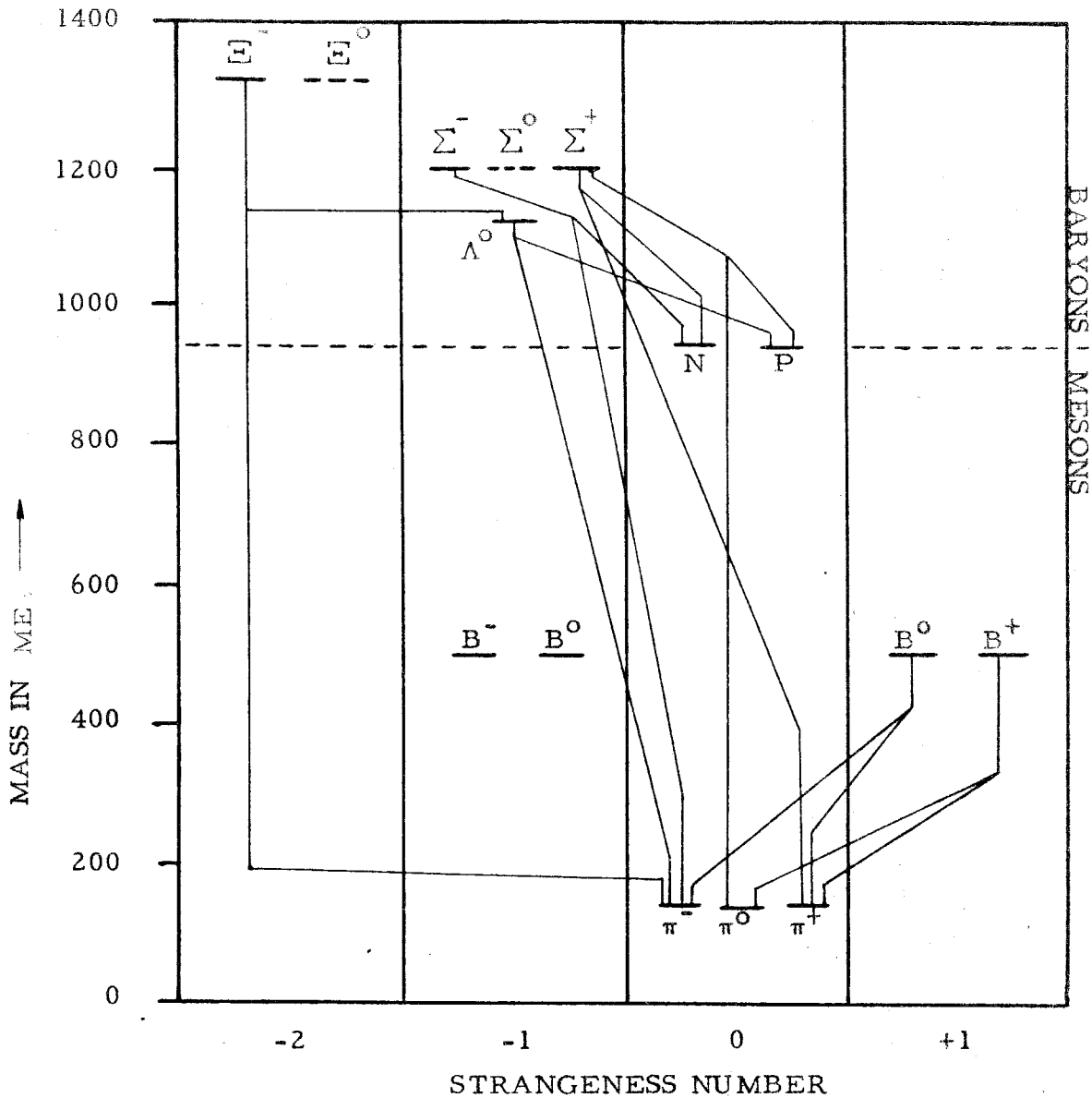


Fig. 9. Mass levels of the Gell-Mann scheme. The mass of each particle is plotted vs. its strangeness number. In slow decay, baryons and charge are conserved, while the total strangeness number changes by  $\pm 1$ . Some observed decay channels are shown.

In 16 of these cases, geometrical measurements indicate that the planes of decay apparently contain a common origin, within errors of measurement. Then the possibility remains that four-fifths of the observed double  $V^0$  events may have been examples of associated production.

Due to large volume and high magnetic field, the 48-inch magnet cloud chambers are better instruments for the detection of double events than earlier smaller devices. In the C. I. T. 18-inch chamber, the number of double events seemed to be no greater than that which could be accounted for through single production alone<sup>(32)</sup>. In about 4,000 penetrating showers, a total of 134  $V^0$  particles were observed, or about 1  $V^0$  in 33 pictures. Only 3 cases showed 2  $V^0$  decays and 1 case showed 3  $V^0$  decays. However, in the 18-inch apparatus the probability of a produced  $V^0$  decaying within the chamber is so small that it would be difficult to observe associated production whether it is the general rule or not.

Another great advantage of the larger chambers and the higher magnetic field is the increased probability of identification of the particle types. In one-half of the 48-inch double  $V^0$  cases, identifications are possible for both events.

Geometrical data and identifications for the 16 double  $V^0$  cases are given in Table I. The identifications are based on the assumption that all observed  $V^0$  events must be either  $\Lambda^0$  or  $\theta^0$  events. Under this limitation, it is easier to identify a  $\theta^0$  than a  $\Lambda^0$  for two reasons:

(a)  $P \sin \theta_T < 118 \text{ Mev}/c$  for all  $\Lambda^0$  decay, and

(b)  $\alpha > 0$  if the  $\Lambda^0$  momentum is greater than  $300 \text{ Mev}/c$ .\*

If either one of these conditions does not hold, the event is identified as a  $\theta^0$ . If both of these conditions do hold, other means must be used to identify the event.

If the mass of the positive track can be estimated from ionization and momentum, the identification is immediate. For masses above  $600 m_e$ , the case is identified as a  $\Lambda^0$ . For masses below  $600 m_e$ , it is identified as a  $\theta^0$ .

Proceeding in this way, it is possible that some of the events listed as  $\theta^0$  are actually  $\tau^0$  or anomalous  $\theta^0$ . With this reservation, the 16 double  $V^0$  events are identified in Table VI.

If associated production of  $\Lambda^0 - \theta^0$  pairs does not occur in the lead absorbers around the 48-inch chambers, one would expect to find that some of the double- $V^0$  decays consist of  $\Lambda^0 - \Lambda^0$  pairs,  $\theta^0 - \theta^0$  pairs, or  $\Lambda^0 - \theta^0$  pairs due to either multiple or plural production. The data admits this possibility, for 8 cases could be  $\theta^0 - \theta^0$  pairs, and 2 cases could be  $\Lambda^0 - \Lambda^0$  pairs. However, every case found to date, where both  $V^0$  particles can be identified, has been the  $\Lambda^0 - \theta^0$  type. There is no obvious bias in the identification procedures which would favor the identification of both particles only in the case of  $\Lambda^0 - \theta^0$  pairs. It is likely, therefore, that associated production of the  $\Lambda^0 - \theta^0$  pairs occurs in cosmic ray penetrating showers in lead.

---

\*If the  $\Lambda^0$  has a momentum less than  $300 \text{ Mev}/c$ , it can be identified from the ionization and momentum of its positive secondary.

Since the origin of a penetrating shower in a cloud chamber ordinarily does not occur in the cloud chamber gas itself, but rather in some nearby dense absorber, a large number of secondary interactions may take place near the origin. Therefore, in order to determine which interaction produced the V-events, it would be desirable for the errors in measurement of the coplanarity of the origin with the decay planes to be as small as possible. However, if no high momentum shower secondaries are available, or if the shower is very dense, the probable error in location of the origin will be high. In Table VI, assigned errors in measurement of the noncoplanarity angles which the assumed origin makes with the decay planes are given with the measured angles ( $\delta$ ) for each case. The measured angles are zero within the stated probable experimental errors except in two border line cases out of 27 measurements. There is no reason to suspect that nearby origins producing  $V^0$  particles singly are responsible for the apparent associated production of  $\Lambda^0 - \theta^0$  pairs.

The angles between the decay planes and production planes are plotted in Fig. 10 in the following way. The smaller angle ( $\eta$ ) is plotted vs. the larger angle for each double  $V^0$  event. All cases are constrained to lie to the right of the heavy line at  $45^\circ$  to the abscissa, and for an isotropic decay, the underlying distribution would be uniform. Strong anisotropy is not indicated by the data.

Even if a polarization of  $V^0$  spins should exist near the point of associated  $V^0$  production, interactions of the  $V^0$  particles before decay could destroy the evidence of this polarization. Since these double  $V^0$  events are produced in a nucleus of a high atomic number,

there is opportunity for  $V^0$  interactions within  $10^{-12}$  cm of their origin. In order to eliminate this difficulty, it would be desirable to use a producing layer of hydrogen.

Some particularly interesting photographs of double  $V^0$  events have been obtained from the 48-inch apparatus. In one event, (Fig. 11) a  $\Lambda^0$  and  $\theta^0$  appear by themselves, apparently produced by a single particle. However, the production dynamics is not consistent with the production of only these two secondaries. Other neutral particles produced at the origin of the  $\Lambda^0$  and  $\theta^0$  could have passed out the front of the chamber without traversing any part of the sensitive region.

In another example, Fig. 12, a star in the gas is the origin of a  $\Lambda^0 - \theta^0$  pair.

Table VI. Geometrical Data for Double  $V^0$  Decays.

1 Event	2 $\delta$	3 $\phi$	4 $\xi$	5 $\eta$	6 Ident.
5802 A <sup>a</sup>	.1+3 <sup>o</sup>	13.3 <sup>o</sup>	69.4 <sup>o</sup>	41.7+5 <sup>o</sup>	$\Lambda^o$
B	.1 $\overline{+}$ 1			28.0 $\overline{+}$ 6	$\theta^o$
27552 A	6.6+5	.8 <sup>+3</sup>	34.3	----- <sup>b</sup>	$\Lambda^o$
B	.3 $\overline{+}$ 4	-.8		-----	$\theta^o$
16460 A	.0+10	40.1	85.3	34.6+10	$\Lambda^o$
B	.0 $\overline{+}$ 3			59.0 $\overline{+}$ 6	$\theta^o$
7604 A	.2+1	8.5	68.2	79.2+5	$\Lambda^o$
B	.3 $\overline{+}$ 2			17.8 $\overline{+}$ 5	$\theta^o$
20232 A	.5+1	19.3	59.8	12.0+3	$\Lambda^o$
B	.4 $\overline{+}$ 2			70.5 $\overline{+}$ 3	$\theta^o$
29431 A	2.7+4	48.5	62.4	41.2+6	$\Lambda^o$
B	3.1 $\overline{+}$ 3			83.0 $\overline{+}$ 12	$\theta^o$
40228 A	.0+0 <sup>c</sup>	14.3	32.3	24.3+20	$\Lambda^o$
B	3.5 $\overline{+}$ 3			55.4 $\overline{+}$ 20	$\theta^o$
16003 A	1.5+2	52.2	54.3	80.0+4	$\Lambda^o$
B	.5 $\overline{+}$ 5			83.3 $\overline{+}$ 4	$\theta^o$
40222 A	----- <sup>d</sup>	22.8	86.5	65.6+7	-
B	-----			29.9 $\overline{+}$ 7	$\theta^o$
24746 A	3.4+3	5.2	7.1	38.3+15	-
B	.3 $\overline{+}$ 3			36.6 $\overline{+}$ 15	$\theta^o$
16393 A	3.0+3	4.3	85.4	59.4+9	-
B	.0 $\overline{+}$ 3			27.1 $\overline{+}$ 9	$\theta^o$
3880 A	2.2+3	21.2	48.2	29.5+12	-
B	2.6 $\overline{+}$ 3			75.6 $\overline{+}$ 9	$\theta^o$
34007 A	1.2+2	18.4	9.0	11.4+4	-
B	.4 $\overline{+}$ 5			6.0 $\overline{+}$ 4	$\theta^o$
33509 A	----- <sup>d</sup>	6.6	57.2	15.2+5	-
B	-----			72.4 $\overline{+}$ 5	$\theta^o$
27009 A	.5+4	5.6	88.8	69.7+7	-
B	2.3 $\overline{+}$ 3			23.2 $\overline{+}$ 12	-
9813 A	2.2+5	5.4	16.6	84.3+9	-
B	1.1 $\overline{+}$ 5			68.9 $\overline{+}$ 9	-

Symbols:

- $\delta$  Angle of noncoplanarity with assumed origin.
- $\phi$  Angle between lines of flight of both  $V^0$  particles.
- $\xi$  Angle between  $V^0$  decay planes.
- $\eta$  Angle between decay plane and plane containing lines of flight of both  $V^0$  particles.

Notes:

- a. Another event which appears to be an anomalous  $\theta^0$  appears in the same shower with 5802 A and B. The shower origin is not coplanar with the tracks of the anomalous  $\theta^0$ .
- b. Since  $\phi$  is zero within experimental error, it is impossible to determine the  $\eta$  angles.
- c. The origin for this case is taken to be the point of intersection of the assumed primary and the line of flight of the  $\Lambda^0$  calculated from the momenta of the  $\Lambda^0$  decay secondaries.
- d. In these cases, the lines of flight of both  $V^0$  particles determined from the momenta of the decay secondaries intersect within experimental error, but there is no other evidence of the origins. Therefore, the intersection of lines of flight are assumed to be the points of production, and no noncoplanarity angles exist.



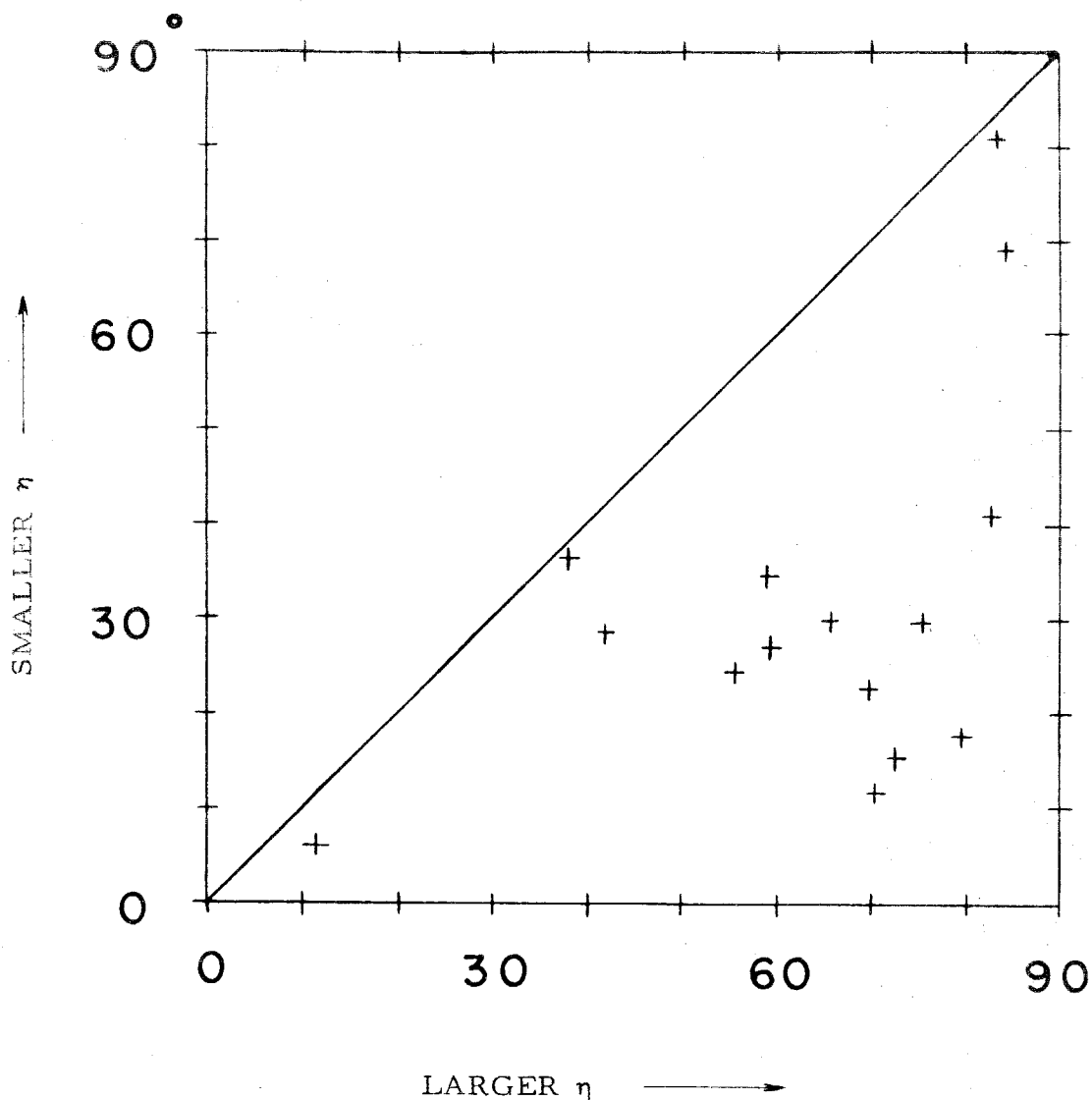


Fig. 13. Angular correlation plot for double  $V^0$  decay. The smaller  $\eta$  is plotted vs. the larger  $\eta$  for each of 15 double  $V^0$  events. The angle  $\eta$  is measured between one decay plane and the plane containing the lines of flight of both  $V^0$  particles. Thus, there are two  $\eta$  angles for each double  $V^0$ -event.

Captions to Figures of Part 3B

Fig. 11. Example of associated production of  $\Lambda^0$  and  $\theta^0$  from an interaction in lead. A primary of  $> 4$  Bev/c momentum passes through chamber 3 and interacts in the lead absorber between chambers 3 and 4. Two  $V^0$  particles produced in this interaction decay in chamber 4. One of them decays into a light negative particle (B) and a heavy positive particle consistent with a proton (C). The other decays into a very fast particle (D) and a slow light particle consistent with a  $\pi^+$  (E). The unstable neutral particles are therefore identified as  $\Lambda^0$  and  $\theta^0$  respectively. Since the interaction took place near the front glass of the chambers, other charged particles produced in this interaction may not have passed through the sensitive region of chamber 4. In fact, the momenta of the  $\Lambda^0$  and  $\theta^0$  do not satisfy the dynamics of any two body collision by a meson or nucleon on a nucleon at rest. Other particles must have been involved.

Fig. 12. Example of associated production of a  $\Lambda^0$  and  $\theta^0$  from a star in the cloud chamber gas. The intersection of the two lines marked (0) gives the position of the star origin. A heavy track consistent with a proton (A) and a light track consistent with a meson (B) appear to be the secondaries of a  $\Lambda^0$  decay. Tracks (C) and (D) apparently come from a  $\theta^0$  decay, for the  $\alpha$  and  $P_{\perp} \sin_T$  values are not consistent with a  $\Lambda^0$ . The lines of flight of both the  $\Lambda^0$  and  $\theta^0$  pass

through the star origin within experimental error.  
There are apparently no other satisfactory origins  
above the chamber.

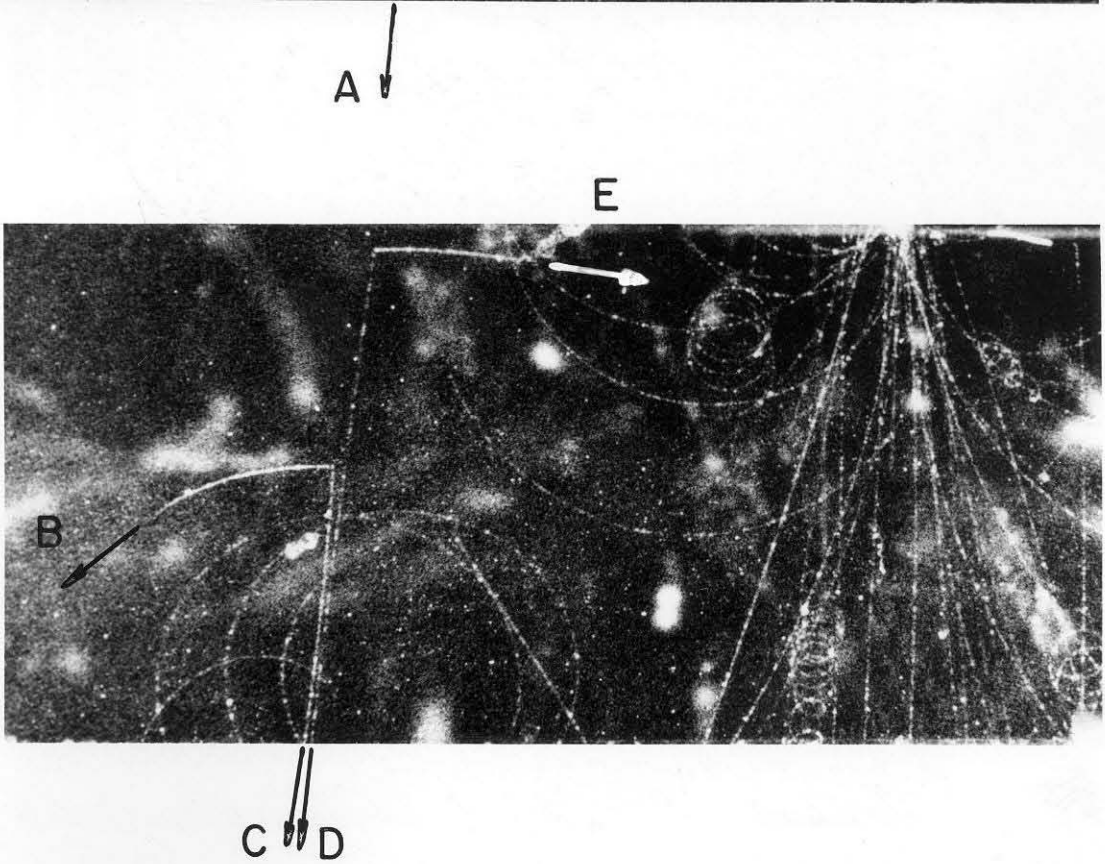
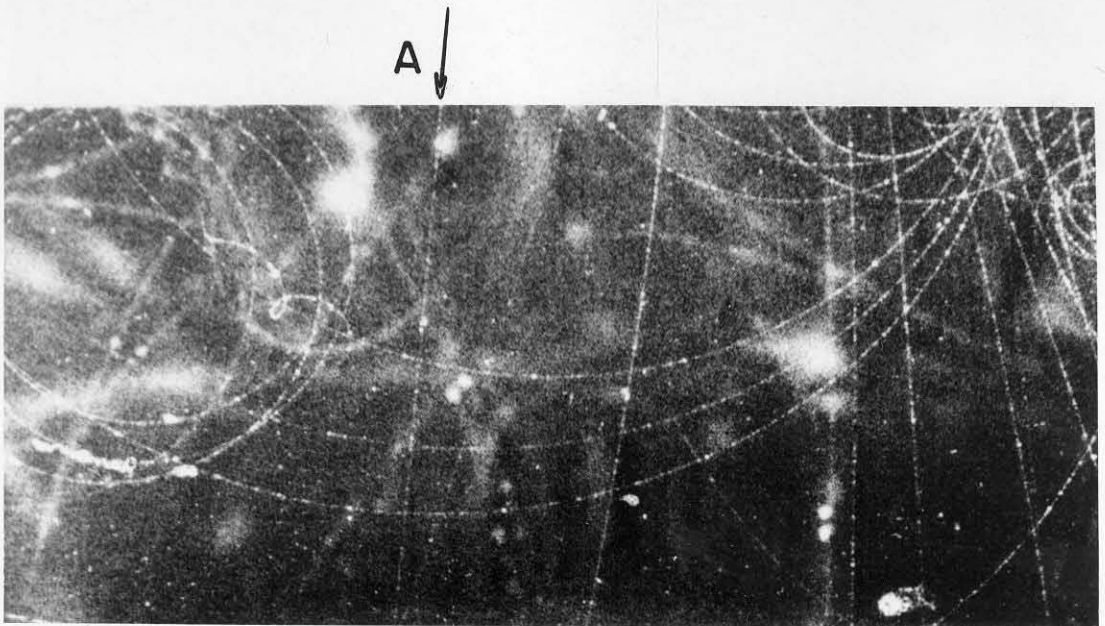


FIGURE II

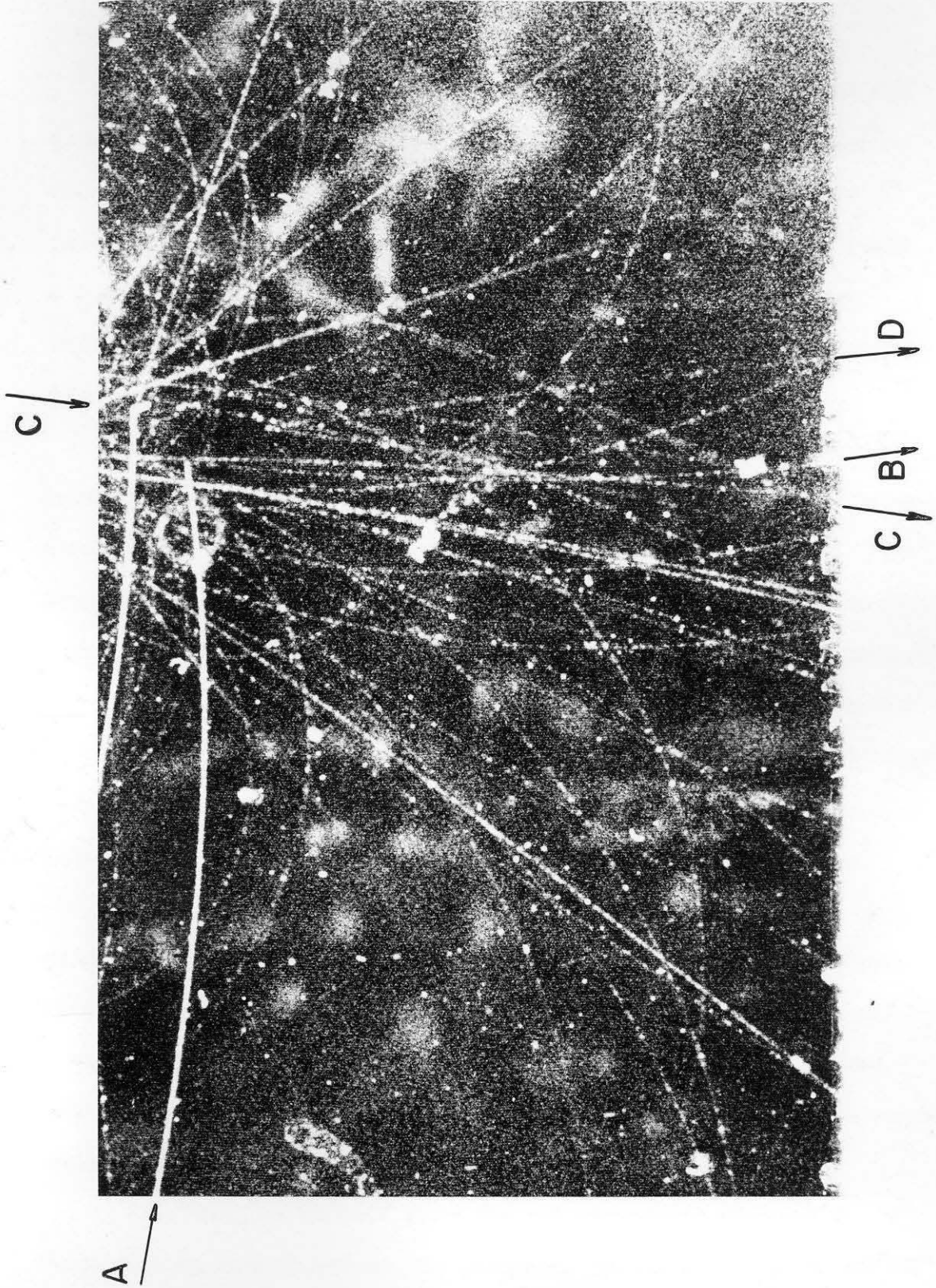


FIGURE 12

### 3 D. TYPES OF ASSOCIATIONS OBSERVED

Table VII lists all of the double V cases found in the 48-inch data through the routine survey for single V events. In addition to the 16 double  $V^0$  events already discussed, there are five  $V^+ - V^0$  cases, three  $V^- - V^0$  cases, and two cases where a  $V^0$  occurs with a charged V of undetermined sign. Examples of the above are shown in Fig. 13 and 14. Not one example of two charged V events in a single chamber has been observed.

A consistent classification of the produced particles can be made in a very simple way through the Gell-Mann scheme. The entire sample of  $V^0 - V^0$  events are consistent with associated  $\Lambda^0 - \theta^0$  production. Therefore, as suggested before<sup>(22)</sup>, the  $\theta^0$  may be the same as the neutral boson of + 1 strangeness in Gell-Mann's scheme.

In the three  $V^- - V^0$  cases, all of the  $V^0$  events are identified as  $\theta^0$  particles. Therefore, a fit is obtained with the Gell-Mann scheme if we assume simply that the  $V^-$  particles observed were hyperons.

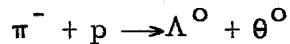
The five  $V^+$  particles were observed with one  $\Lambda^0$  and four unidentified  $V^0$  events, all of which have positive  $\alpha$ -values. Therefore one suspects that the majority of  $V^+$  may have been produced with  $\Lambda^0$ . Under Gell-Mann's scheme, the  $V^+$  could be identical with the positive boson, which we will call  $\theta^+$ . Its strangeness would indeed be opposite to that of the  $\Lambda^0$  and  $\Sigma^-$ .

Nothing can be said about the two remaining charged V -  $V^0$  cases for no identifications are possible. Of course, the  $\Xi^- + \theta^0 + \theta^0$  case described in Part II is compatible with the general scheme, for the  $\Xi^-$  is assigned a strangeness of -2, and the  $\theta^0$  particles

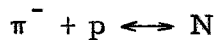
have strangeness of +1 each.

We have not found any cases which need concern  $\Xi^0$ ,  $\Sigma^0$ ,  $\Sigma^+$ , or  $\theta^-$  ( $B^-$ ) in the double V cases, though such events will possibly be found soon in the 48-inch apparatus. The identity of the anti-boson is also undetermined.

The  $\theta^0$  cannot have the same strangeness as the anti- $\theta^0$  under the Gell-Mann scheme because strangeness changes sign under charge conjugation. This result is compatible with rather direct experimental evidence as shown by Gell-Mann and Pais. (33) From the fast production process



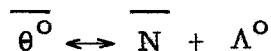
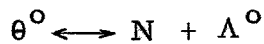
and the strong Yukawa interaction



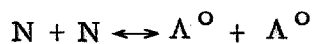
we may infer that the virtual process



is fast. Denoting anti-particles by a bar, the above requires that



be fast virtual interactions. If  $\theta^0$  and  $\overline{\theta^0}$  were identical, then



would be a fast process. Since this production process has not been observed, we conclude that



Gell-Mann and Pais have shown that this fact leads to other peculiar relationships. Since the  $\theta^0$  and  $\overline{\theta^0}$  are distinct, they must be associated with a complex field  $\psi_0$  which transforms under the charge conjugation operator C according to

$$C \psi_0 C^{-1} = \psi_0^+ \quad \text{and}$$

$$C \psi_0^+ C^{-1} = \psi_0$$

where  $\psi_0^+$  differs from its Hermetian conjugate,  $\overline{\psi_0}$ . The  $\theta^0$  is associated with  $\psi_0$ , and  $\overline{\theta^0}$  with  $\psi_0^+$ . If we define

$$\psi_1 = \frac{(\psi_0 + \psi_0^+)}{\sqrt{2}} \quad \text{(a)}$$

and

$$\psi_2 = \frac{(\psi_0 - \psi_0^+)}{\sqrt{2} i} \quad \text{(b)}$$

so that  $\psi_1$  and  $\psi_2$  are Hermetian field operators, then

$$C \psi_1 C^{-1} = \psi_1$$

$$C \psi_2 C^{-1} = -\psi_2$$

which indicate that  $\psi_1$  is even and  $\psi_2$  is odd under charge conjugation. Furthermore, from (a) and (b), the creation of a  $\theta^0$  corresponds to the creation with equal probability of either a  $\theta_1$ , or  $\theta_2$ , the quanta associated with the  $\psi_1$  and  $\psi_2$  fields respectively.

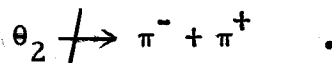
Since these two quanta,  $\theta_1$  and  $\theta_2$ , have the same spin and parity as the  $\theta^0$ , they must decay through different modes, for the  $\theta_1$  must be in a state that is even under charge conjugation and the  $\theta_2$  must be in a state that is odd under charge conjugation. For



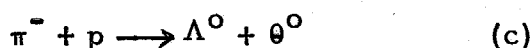
instance, if



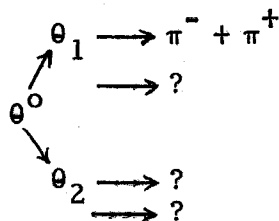
then



The conclusion of Gell-Mann and Pais is that after production through a process such as



the  $\theta^0$  has two or more decays



of which only one has been identified. However, since the above decay mode for  $\theta_1$  is more frequently observed than any other which might correspond to  $\theta_2$  (or  $\theta_1$ ), such as  $\theta_2 \longrightarrow L_- + L_+ + ?$ , where L refers to any light meson, the  $\theta_2$  lifetime should be an order of magnitude longer than that of  $\theta_1$ .

In the 48-inch data there are two clear examples of very anomalous  $\theta^0$  (Table VIII) which might be examples of  $\theta_2$  decays. For one of them, 31855,  $Q(\pi, \pi)$  is only  $10 \pm 1$  Mev. This excellent example occurs with a  $V^+$  decay, but since the  $V^+$  cannot be identified as either a meson or hyperon nothing can be said concerning the possible strangeness of these decays.

The other event, 19143, has been previously reported. (34)  
This anomalous  $\theta^0$  has  $Q(\pi, \pi) \approx 41 \pm 5$  Mev, and the presumed line of flight based on two body decay would pass through the origin of no apparent nuclear interaction. It is accompanied by a normal  $\theta^0$  in the same penetrating shower.

Table VII. Multiple V-events observed in a single cloud chamber of the 48-inch apparatus (March 1, 1955).

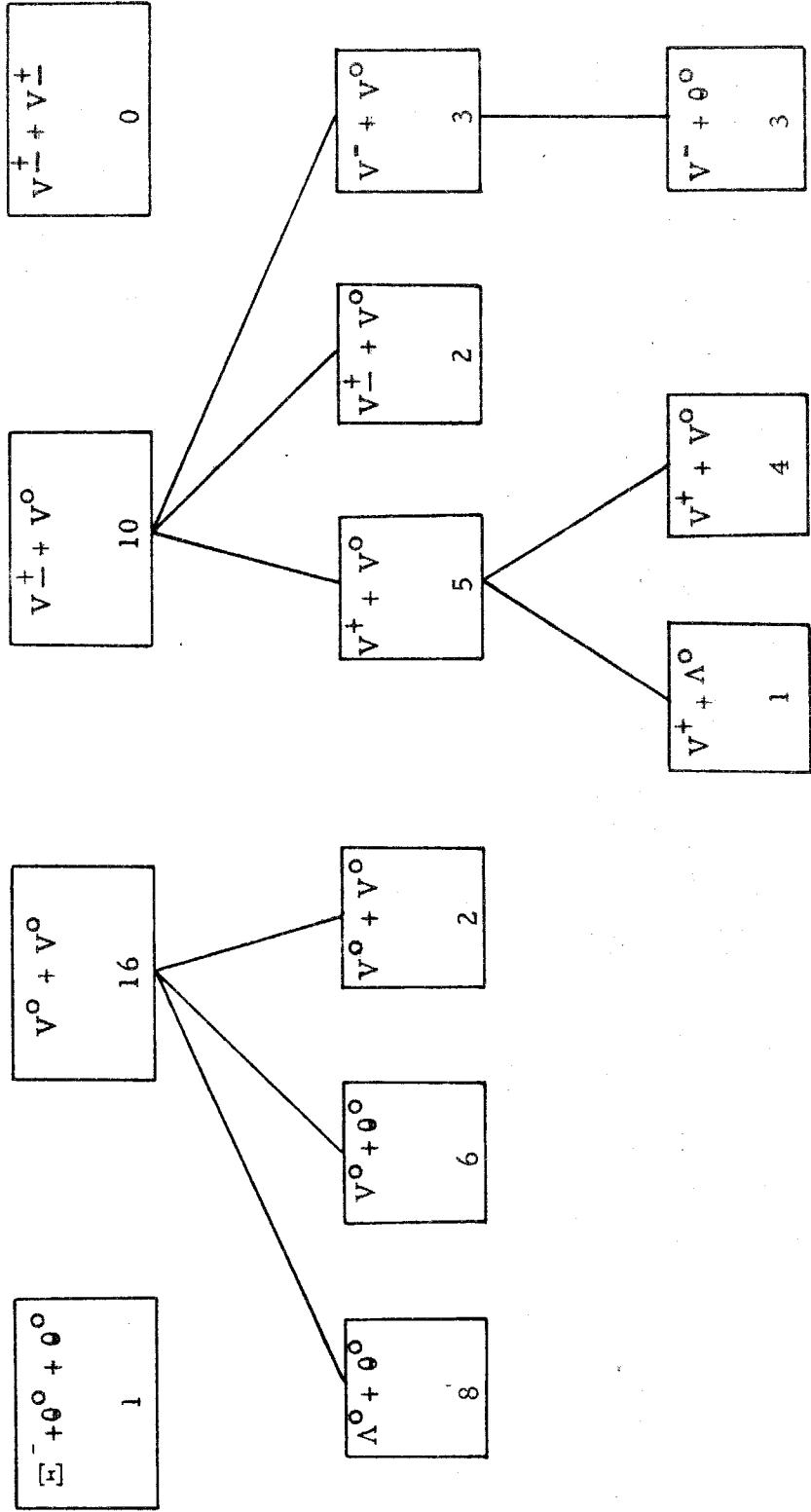


Table VIII. Very anomalous  $\theta^0$  observations.

Event	Secondary	Momentum Mev/c	Ionization times minimum	Mass $m_e$	Angle between secondaries	$Q(\pi, \pi)$ Mev
19143	+	$260 \pm 20$	1 - 2	< 640	$40^\circ$	$41 \pm 5$
	-	$87 \pm 4.5$	1.5 - 3	160 - 300		
31855	+	$156 \pm 5$	1 - 2	< 400	$27.3^\circ$	$10 \pm 1$
	-	$86 \pm 6$	1 - 2	< 240		

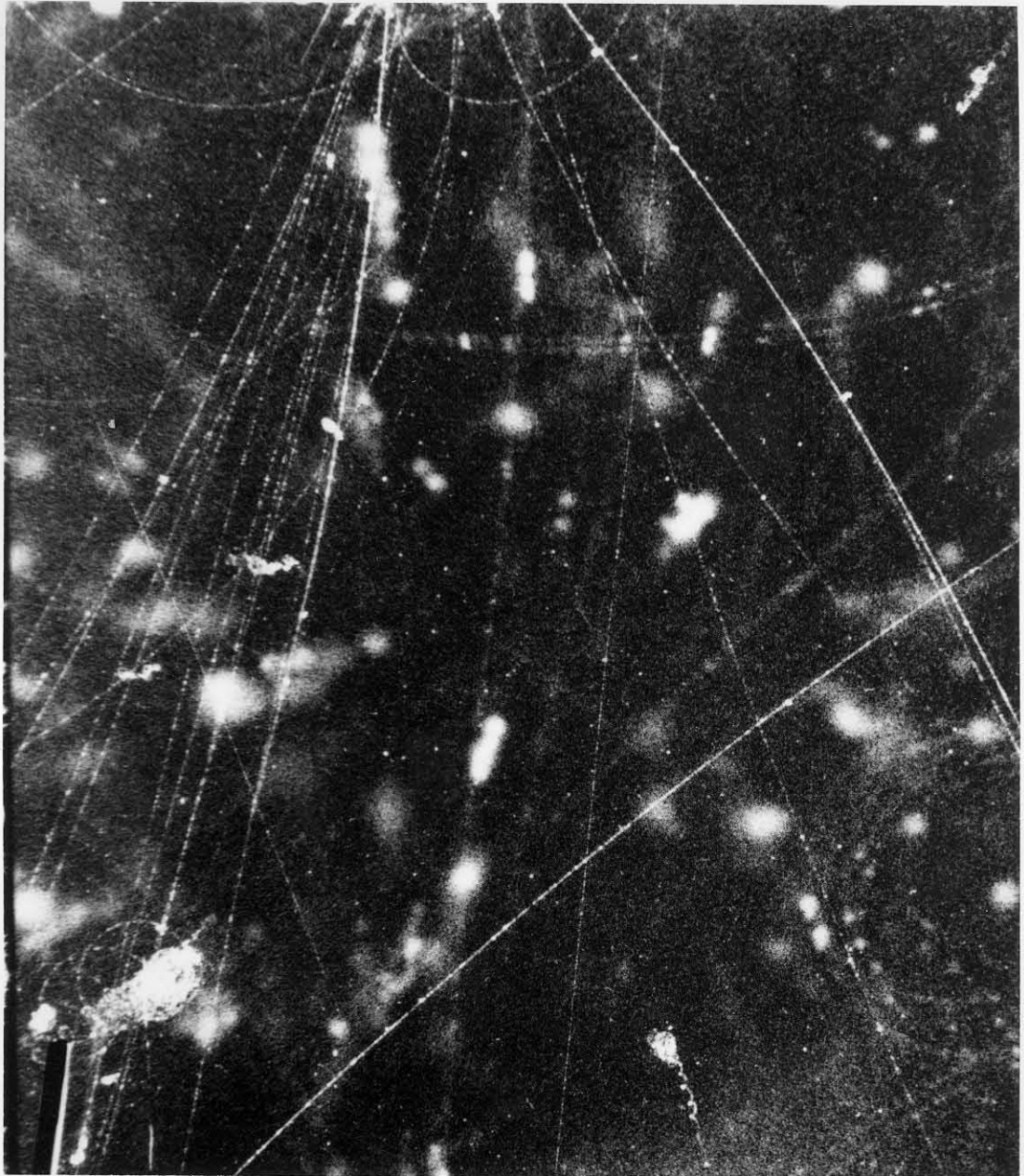
Caption to Figures of Part 3D

Fig. 13. An example of a  $V^+ - V^0$  event. The decay of the  $V^+$  takes place at the intersection of tracks (A) and (B). The  $V^0$  event (C-D) is consistent with either a  $\Lambda^0$  or  $\theta^0$ .

Fig. 14. An unusual example of the associated production of a  $V^-$  with a  $\theta^0$  from a star in the chamber gas. The  $\theta^0$  is immediately identified from the high momentum of the negative secondary and the large angle of the decay. The ionization and momentum of the positive secondary are also characteristic of a light meson.

A/

B/



C

D

FIGURE 13

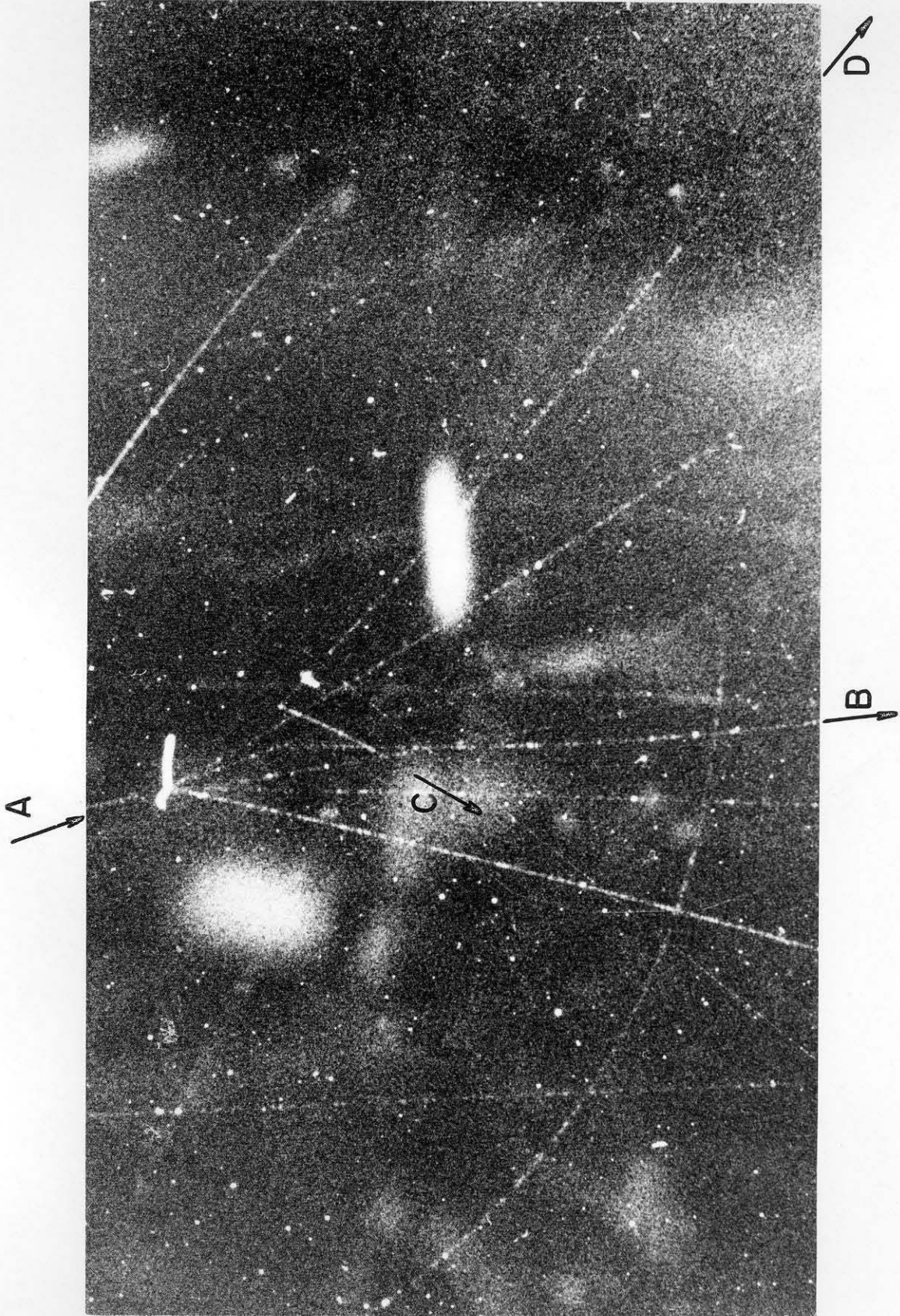


FIGURE 14

REFERENCES

Part 1

1. V. A. J. Van Lint, G. H. Trilling, R. B. Leighton, and C. D. Anderson, *Phys. Rev.* 95, 295 (1954); V. A. J. Van Lint, C. D. Anderson, E. W. Cowan, R. B. Leighton, and C. M. York, Jr., *Phys. Rev.* 94, 1732 (1954); G. H. Trilling and R. B. Leighton, to be published in *Phys. Rev.*
2. G. H. Trilling, Thesis, California Institute of Technology, 1955.
3. V. A. J. Van Lint, Thesis, California Institute of Technology, 1954.
4. M. Danysz and J. Pniewski, *Phil. Mag.* 44, 348 (1953).
5. D. A. Tidman, G. Davis, A. J. Herz, and R. M. Tennent, *Phil. Mag.* 44, 350 (1953).
6. J. Crussard and D. Morellet, *Comptes Rendus* 236, 64 (1953).
7. M. W. Friedlander, D. Keefe, M. G. Menon, and M. Merlin, *Phil. Mag.* 45, 533 (1954).
8. G. Lovera, L. B. Silva, C. Bonacini, C. DePietri, R. P. Fedeli and A. Roveri, *Nuovo Cimento* 10, 986 (1953).
9. P. S. Frier, G. W. Anderson, and J. E. Naugle, *Phys. Rev.* 94, 677 (1954).
10. R. D. Hill, E. O. Salant, M. Widgoff, L. S. Osborne, A. Pevsner, D. M. Ritson, J. Crussard, and W. D. Walker, *Phys. Rev.* 94, 797 (1954).
11. A. Bonetti, R. Levi Setti, M. Pavetti, L. Searsi, G. Tomasini, *Nuovo Cimento* 11, 210 (1954); A. Bonetti, K. Levi Setti, M. Pavetti, L. Searsi, G. Tomasini, *Nuovo Cimento* 11, 330 (1954).



12. W. F. Fry and G. R. White, *Nuovo Cimento* 11, 551 (1954).
13. P. H. Barrett, *Phys. Rev.* 94, 1328 (1954).
14. A. Solheim and S. O. Sorensen, *Phil. Mag.* 45, 1284 (1954).
15. H. Yagoda, *Phys. Rev.* 98, 153 (1955).
16. A. Debenedetti, C. M. Garelli, G. Lovera, L. Tallone, and M. Vigone, *Nuovo Cimento* 12, 466 (1954).
17. B. Waldeskog, *Ark. Fys.* 8, 369 (1954).
18. J. E. Naugle, E. P. Ney, P. S. Freier, and W. B. Cheston, *Phys. Rev.* 96, 1383 (1954).
19. W. F. Fry and M. S. Swami, *Phys. Rev.* 96, 809 (1954).
20. W. F. Fry, J. Schneps, and M. S. Swami, *Phys. Rev.* 97, 1189 (1955).

### Part 2

21. W. H. Arnold, J. Ballam, G. K. Lindeberg, and V. A. J. Van Lint, *Phys. Rev.* 98, 838 (1955); W. B. Fretter and F. W. Friesen, *Phys. Rev.* 96, 853 (1954); E. W. Cowan, *Phys. Rev.* 94, 161 (1954).
22. M. Gell-Mann, *Phys. Rev.* 92, 833 (1953); M. Gell-Mann and A. Pais, *Proceedings of the Glasgow Conference*, 1954; M. Gell-Mann, *On the Classification of Particles* (circulated in preprint form, August, 1953); M. Gell-Mann, *The Interpretation of the New Particles as Displaced Charge Multiplets*, (*Proc. of Pisa Conference*, 1955).

### Part 3

23. G. D. Rochester and C. C. Butler, *Nature* 160, 855 (1947).

24. R. B. Leighton, S. D. Wanlass, and C. D. Anderson, Phys. Rev. 89, 148 (1953).
25. Unpublished.
26. Y. Nambu, K. Nishijima, and Y. Yamaguchi, Prog. Theor. Phys. 6, 615 and 619 (1951).
27. W. B. Fowler, R. P. Shutt, A. M. Thorndike, and W. L. Whittemore, Phys. Rev. 91, 1287 (1953); Phys. Rev. 93, 861 (1954); and Phys. Rev. 98, 121 (1955).
28. R. W. Thompson, J. R. Burwell, R. W. Huggett, and C. J. Karzmark, Phys. Rev. 95, 1576 (1954); J. D. Sorrels, Proceedings of the Fifth Annual Rochester Conference, January 1955.
29. D. Lal, Y. Pal, and B. Peters, Proc. Ind. Acad. of Sci. 38, 398 (1953); C. Dahanayake, P. E. Francois, Y. Fujimoto, P. Iredale, C. J. Waddington, and M. Yasin, Phil. Mag. 45, 855 (1954).
30. S. B. Treiman, G. T. Reynolds, and A. L. Hodson, Phys. Rev. 97, 244 (1955); J. Ballam, A. L. Hodson, W. Martin, R. Ronald Rau, G. T. Reynolds, and S. B. Treiman, Phys. Rev. 97, 245 (1955). The data presented in the latter paper was considerably modified as presented before the Fifth Annual Rochester Conference, January, 1955.
31. As pointed out by Treiman (Ref. 30, above), particles of spin one-half must also decay isotropically, for reasons of parity and angular momentum conservation.
32. R. B. Leighton, S. D. Wanlass, and C. D. Anderson, Phys. Rev. 89, 148 (1953).

33. M. Gell-Mann and A. Pais, Phys. Rev. 97, 1387 (1955).
34. V. A. J. Van Lint, C. D. Anderson, E. W. Cowan, R. B. Leighton, and C. M. York, Jr., Phys. Rev. 94, 1732 (1954).
35. K. Nishijima, Prog. Theor. Phys. 13, 285 (1955).